chemosensors

MDPI

Review

Lanthanide-Doped Upconversion Luminescence: A New Frontier in Pathogenic Bacteria and Metabolite Detection from Design to Point-of-Care Application

Huanhuan Li [1,*], Yu Wu [1,2], Muhammad Shoaib [1], Wei Sheng [1], Qiyi Bei [1] and Arul Murugesan [1]

[1] School of Food and Biological Engineering, Jiangsu University, Zhenjiang 212013, China; 15536453131@163.com (Y.W.); shoaibbema@gmail.com (M.S.); 2222218040@stmail.ujs.edu.cn (W.S.); 1004tjw@gmail.com (Q.B.); chemarul91@gmail.com (A.M.)
[2] Faculty of Agricultural Engineering, Jiangsu University, Zhenjiang 212013, China
* Correspondence: lhhrhf@163.com; Tel.: +86-511-88790318; Fax: +86-511-88780201

Abstract: Pathogens and their metabolites in food present significant risks to both human health and economic development. Rising living standards and increasing awareness of food safety have driven the demand for sensitive and rapid detection methods. Lanthanide-doped upconversion nanoparticles (UCNPs), with their exceptional optical properties, have emerged as a promising platform for developing biosensors to detect pathogenic bacteria and their metabolites. The integration of UCNPs with point-of-care testing (POCT) has garnered considerable attention for its portability and immediacy, highlighting a promising future for biosensing, particularly in applications requiring quick and accurate diagnostics. This review explores the recognition elements and design principles commonly used in UCNP-based biosensors and examines various applications, including lateral flow assays, microfluidic systems, photoelectrochemical devices, and smartphone-integrated platforms. Despite significant advancements, challenges remain in the applicability and commercialization of UCNP-based biosensing technology. Future research should focus on enhancing sensitivity and specificity, developing scalable and cost-effective production methods, and integrating with advanced digital technologies to enable broader adoption. Addressing these challenges, establishing regulatory frameworks, and considering sustainability will be crucial to fully realizing the potential of UCNP-based biosensors.

Keywords: lanthanide-doped upconversion nanoparticles; pathogens; metabolites; point-of-care; food safety

check for updates

Received: 31 December 2024
Revised: 3 February 2025
Accepted: 5 February 2025
Published: 8 February 2025

Citation: Li, H.; Wu, Y.; Shoaib, M.; Sheng, W.; Bei, Q.; Murugesan, A. Lanthanide-Doped Upconversion Luminescence: A New Frontier in Pathogenic Bacteria and Metabolite Detection from Design to Point-of-Care Application. *Chemosensors* **2025**, *13*, 60. https://doi.org/10.3390/chemosensors13020060

Copyright: © 2025 by the authors. Licensee MDPI, Basel, Switzerland. This article is an open access article distributed under the terms and conditions of the Creative Commons Attribution (CC BY) license (https://creativecommons.org/licenses/by/4.0/).

1. Introduction

Food is a crucial aspect of everyone's life. The supply and consumption of nutritious and safe food are important for life and consumer health [1,2]. However, foodborne illnesses caused by bacteria and their metabolites, such as *Pseudomonas aeruginosa*, aflatoxin B_1, and botulinum neurotoxins, always remain challenging to ensure food safety and are recognized as a significant public health threat globally [3–8]. The Centers for Disease Control and Prevention (CDC) reports that bacterial infections affect about one in every six Americans annually, leading to 3000 fatalities and incurring costs of approximately $15.6 billion [9]. Meanwhile, these bacteria also produce poisonous substances known as toxins, which possess immuno-toxic, teratogenic, and carcinogenic effects that can easily accumulate in processed foods and persist even at high temperatures. The use and supply of unsafe food affects individuals' health and increases the burden on economies in terms

of high costs and financial loss. The World Bank has estimated an annual loss of 110 billion USD in low- and middle-income economies due to productivity loss and higher medical expenses. Therefore, quick, reliable, and sensitive detection is imperative to prevent and control foodborne illnesses.

Until now, many technologies have been utilized to detect pathogenic bacteria and their metabolites. These technologies can be divided into chromatographic- and spectrometric-based assays, polymerase chain reaction (PCR), colony-counting methods, and enzyme-linked immunosorbent assay (ELISA). The chromatographic- and spectrometric-based assays have high sensitivity and selectivity but require well-equipped laboratories and trained personnel [10–12]. Culture-based methods need additional enrichment processes to amplify bacterial counts for detectable levels, and PCR assays demand sophisticated instrumentation, intricate operating procedures, and costly reagents. That is why their reliability is compromised by the frequent occurrence of false positive results, which arise from the amplification of dead cells and human errors. ELISA relies on the existence of specific antibodies, which are difficult to produce and require an immune response from animals. Their higher cost, shorter shelf life, more batch-to-bath variations, and instability hinder the growth and application of ELISA-based methods [13,14]. In this regard, easy-to-operate, rapid, cheap, and sensitive alternative approaches are required to detect foodborne pathogens and their metabolites on-site.

With recent advancements in modern technology, nanotechnology applications have surged. Due to its high performance and diverse properties, nanotechnology shows great promise for enabling the sensitive, selective, and straightforward detection of food-related bacteria and their byproducts. Compared with traditional technologies, nanotechnology overcomes the limitations of conventional methods, such as slow, laborious, complicated processes and requirements of expensive instruments. The advancements in nanotechnology have driven the exploration, innovation, and application of nanomaterials. Various nanomaterials are utilized in electrochemical and surface-enhanced Raman spectroscopy (SERS) sensing techniques, providing significant advantages such as speed, sensitivity, precision, and cost-effectiveness [15,16]. However, the electrode's strict humidity and temperature requirements limit their real-time application in electrochemical methods. SERS also becomes unworthy owing to its sophisticated data analysis, high instrument costs, and heterogeneous and complex nature of the real sample. Besides that, luminescence nanoparticles have excellent attributes, including photoluminescence, emission, and size dependence, enhancing food analysis's sensitivity, selectivity, and accuracy.

In the field of luminescent nanomaterials, traditional down-conversion fluorescent materials, including semiconductor nanoparticles, dye-linked hybrid systems, and mesoporous silica, are widely utilized in biological research and clinical applications for their distinctive properties. However, the notable inherent drawbacks include the typical emission of a single photon of lower energy after absorbing a high-energy photon in the ultraviolet/visible spectra. These drawbacks include limited light penetration depth, the risk of causing severe harm to living organisms due to photodamage, and the presence of autofluorescence (or noise) in certain biological samples. There has been a significant interest in advancing upconversion technology to overcome these challenges, primarily because of the distinct luminescence characteristics of upconversion nanoparticles.

Since the first observation of the upconversion phenomenon in 1959 and the proposal of the upconversion concept in 1966, over the last decade, the fluorescence technology based on upconversion nanoparticles has considerably matured, as shown in Figure 1 [1,17–19]. Due to the addition of rare-earth elements, upconversion nanoparticles exhibit the ability to upconvert low-energy near-infrared photons into high-energy visible and ultraviolet photons. This results in large anti-Stokes shifts and narrow emission peaks, which help reduce

autofluorescence and enhance penetration power [20]. Commonly used rare-earth elements in upconversion nanoparticles include Er and Tm. Er-doped upconversion nanoparticles typically exhibit their maximum emission peaks at 407, 520, 528, 540, 550, 654, 660, 698, and 842 nm, while Tm-doped upconversion nanoparticles typically show peaks at 450, 474, 645, and 802 nm. Consequently, when employing upconversion nanoparticles to detect targets, their specificity does not rely on the dopant ions and fluorescence wavelength. Generally, upconversion nanoparticles are typically divided into two categories: lanthanide-doped upconversion nanoparticles (UCNPs) and upconversion metal complexes [21]. However, upconversion metal complexes generally exhibit broader emission bands and a lower efficiency compared to UCNPs. This is because UCNPs, which often use $NaYF_4$ as a substrate material, benefit from $NaYF_4$'s low phonon energy environment, enhancing the overall performance of the UCNPs. In addition, UCNPs have unique advantages, including resistance to photobleaching and longer fluorescence lifetimes (on the millisecond scale). These exceptional luminescent properties of UCNPs have triggered a broad application of UCNPs to detect food contaminants [22]. Recently, UCNPs have demonstrated their effectiveness in detecting bacteria and their metabolites.

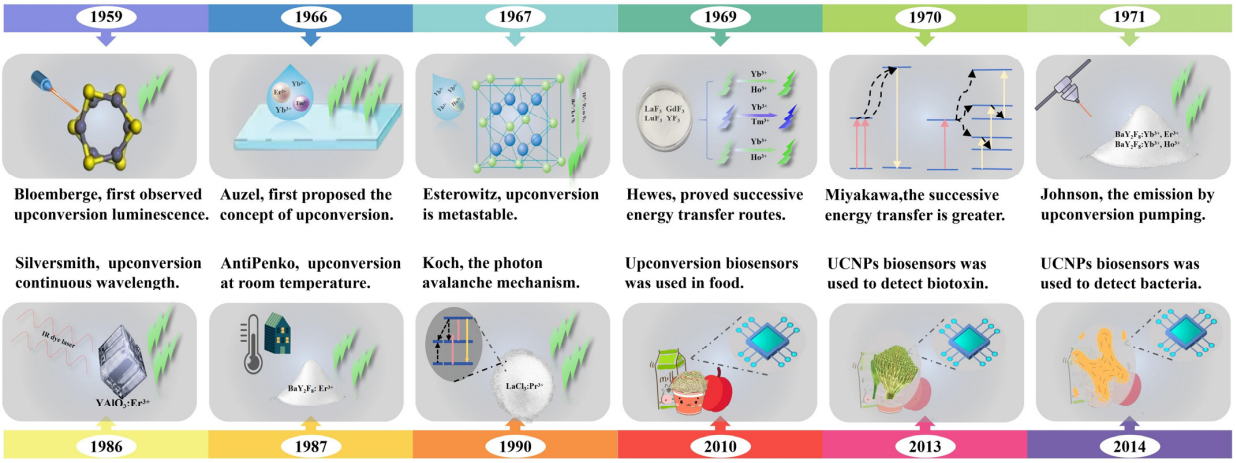


Figure 1. Schematic illustration on the timeline of the development of the UCNPs, especially its application in detecting foodborne bacteria and their metabolites.

Several research papers have been published on the use of UCNPs-based sensors for food safety applications, particularly for detecting various types of food contaminants, such as heavy metal ions and pesticide residues [1,17–19]. The existing literature inadequately summarizes the application of UCNPs in detecting bacteria and their metabolites, and a more comprehensive analysis of portable, on-site systems is needed. This review article addresses this gap by exploring current trends and advancements in using UCNP-based sensors to detect pathogenic bacteria and their metabolites, particularly focusing on portable and on-site applications. Considering the mentioned elements, this review primarily focuses on the latest progress in using UCNPs to identify pathogens and their metabolites in food samples. The discussion begins with a brief overview of various recognition elements, including antibodies, aptamers, molecularly imprinted polymers, and enzymes, followed by an in-depth examination of design strategies for UCNP-based sensing systems, such as fluorescence resonance energy transfer, inner filter effects, magnetic separation techniques, and related mechanisms. These insights from this study are expected to assist researchers in advancing the construction of highly efficient biosensors based on UCNPs. Subsequently, the summarization of a UCNP-based biosensor's applications to detect pathogenic bacteria, including *E. coli*, *L. monocytogenes*, *S. aureus*, and *Salmonella*, as well as their metabolites, such as aflatoxin B_1, ochratoxin, fumonisin B_1, and deoxynivalenol. Furthermore, due to

the remarkable advantages of convenience in limited-resource areas and the conservation of energy and reagents [23], UCNP-based POCT tools, including lateral flow assays, microfluidic, photoelectrochemistry, and smartphones, were emphasized. Finally, we discussed the recent challenges and future prospects of UCNP-based sensing systems for food safety applications, as schematically illustrated in Figure 2.

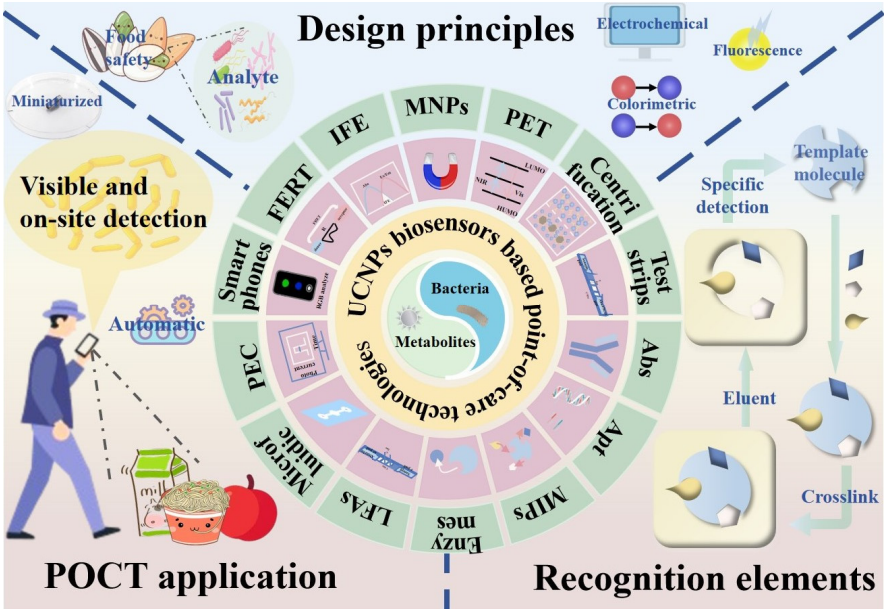


Figure 2. The recent challenges and future prospects of UCNP-based sensing systems for food safety applications.

2. Recognition Elements of UCNP-Based Biosensors

UCNPs act as transducers, transforming energy from near-infrared (NIR) into ultraviolet–visible (UV-vis) light. To achieve the response to target, a UCNP-based biosensor is usually connected to recognition elements. Consequently, UCNPs do not have specificity to their targets, which is neither influenced by the dopant ions, such as Yb, Tm, Yb, or Er, nor by the fluorescence wavelength. In this study, we highlights the diverse recognition elements employed in detecting pathogens and their metabolites, such as antibodies, aptamers, molecularly imprinted polymers, and enzymes (Figure 3), with a summary of their respective advantages and limitations presented in Table 1.

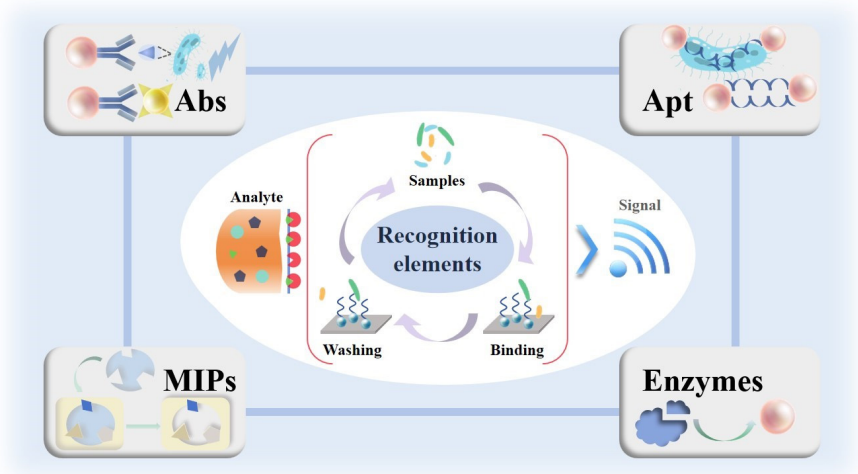


Figure 3. Schematic illustration of recognition elements utilized for constructing UCNP-based biosensors, including Abs, Apts, MIPs, and enzymes.

2.1. Antibodies

Living bodies produce antibodies (Abs)/protective proteins through antigenic stimulation, which possess a high specificity to a particular objective/target [24–26]. Because of the selectivity, many UCNP-based biosensors have been successfully developed with Abs as recognition elements. Abs are usually utilized in immunoassays, including the immunochromatographic assay (ICA), the double-antibody sandwich method [27], the dual-mode immunochromatographic assay (dICA) [28], the photoelectrochemistry immunosorbent assay [29], and the multiplexed fluorescence immunoassay [30]. ICA has attracted a growing interest among these assays due to its simplicity, single-step, straightforward procedure, and faster detection within 10 min. Chen et al. effectively developed a distinct and sensitive ICA capable of detecting zearalenone (ZEN) within 10 min. The developed sensor utilized 20% lanthanum (La^{3+})-doped upconversion nanoparticles as antibody labels in the ICA. The methods improved fluorescence performance and sensitivity. Under optimal conditions, the detection limit for ZEN standard solutions was also 0.25 ng/mL, with CVs of less than 8.67% and a high linear correlation (R^2 = 0.9944). The presence of multiple types of mycotoxins in food samples urges the development of multiplex simultaneous detection systems, which are essential to ensure food safety. Numerous studies have indicated that UCNPs coupled with antibodies are an excellent choice for developing a simultaneous detection system [31]. Also, the authors designed a dual-channel ICA based on the 30% La^{3+}-doped UCNPs to detect aflatoxin B_1 (AFB_1) and ZEN simultaneously in 10 min. The results proved that the developed test strips were highly specific, stable, and matrix tolerant [32–34]. For instance, Zhang et al. designed a dual-color sensor for the simultaneous detection of pathogens (*E. coli* and *S. aureus*) by applying different types of lanthanide-doped UCNPs. The detection probes successfully captured the target bacteria by using antibodies that were precisely linked to them. The fluorescence signals increased proportionally as the count of *E. coli* (664 nm) and *S. aureus* (806 nm) rose, ranging from 47 to 47 × 10^6 cfu/mL (R^2 = 0.98) and 64 to 64 × 10^6 cfu/mL (R^2 = 0.97), respectively. As a result, the limit of detection was relatively low, at 13 cfu/mL for *E. coli* and 15 cfu/mL for *S. aureus*. As proteins, antibodies are highly sensitive to environmental factors like temperature and pH, making them prone to deactivation or degradation. This can lead to inconsistent performance in UCNP-based biosensors. Additionally, regarding their cost, it is essential to improve the production process of antibodies or choose alternative recognition components that can interact with upconversion nanoparticles [35].

2.2. Aptamer

The aptamer is an oligonucleotide sequence of deoxyribonucleic acid (DNA) or ribonucleic acid (RNA) selected through the Systematic Evolution of Ligands by Exponential Enrichment (SELEX) process [36]. Due to the swift advancement in aptamer technology, many researchers use aptamers as a recognition element for developing biosensors. This preference is attributed to its several benefits, which include the following: (I) aptamers have the ability to bind and identify different types of targets, and the affinities range from nanomolar to picomolar [37]; (II) aptamers can be efficiently produced on a large scale in a short period using PCR, ensuring high precision and consistency without the need for immunization or the use of animal hosts [38]; (III) aptamers, in contrast to antibodies, do not require stringent storage and detection conditions for the kits [13]. In addition, aptamer-UCNPs have a higher affinity, specificity, and stability; simpler synthesis and modification processes; and the lowest immunogenicity compared to antibodies [39]. These practical benefits enable the UCNP–aptamer-based sensors to identify different pathogens and their metabolites in food samples effectively. For example, Cheng et al. developed a sensitive aptamer-based sensor for detecting *S. Typhimurium* using Mn^{2+}-doped UCNPs as

the donor and gold nanorods (AuNRs) as the acceptor [40,41]. In another study, a novel aptasensor was developed to detect ZEN in maize samples by using UCNPs as a signal probe and functionalized graphene oxide (FGO) as a quencher [10]. The identification of *S. aureus* (ATCC 29213) was also achieved through a bioassay utilizing UCNPs and aptamers as the donor and the black hole quencher$_1$ (BHQ_1) ligated with cDNA as the acceptor. The sensor successfully utilized fluorescence resonance energy transfer (FRET) at a distance less than 10 nm between UCNPs and BHQ_1. This was made possible by the base pairing of the aptamer and cDNA [42,43]. During the construction phase of the UCNP-based biosensor, utilizing aptamers for recognition is convenient and less restrictive. However, obtaining highly selective aptamers targeting certain bacteria may pose challenges, potentially limiting their practical use for end-users.

2.3. Molecularly Imprinted Polymers

In recent years, molecularly imprinted polymers (MIPs), often referred to as "artificial antibodies", have gained significant attention as exceptional recognition materials. MIPs are highly cross-linked, three-dimensional network polymers synthesized via covalent and non-covalent interactions between target molecules (or their structural analogs), functional monomers, and cross-linking agents [13,44–47]. The binding site's relative positions restrict the conventional MIPs from integration with UCNPs [48,49]. Typically, to give UCNP-based biosensors the capacity to identify and bind bacteria precisely, MIPs are often directly coated onto the surface of UCNPs. This process results in electron transfer (ET), which is then used to cause changes in upconversion luminescence signals upon target binding. For example, Yan et al. designed a biosensor that successfully combined UCNPs and MIPs to detect ochratoxin A (OTA) with high selectivity and specificity. A linear reduction in fluorescence intensity was recorded as the higher concentrations of OTA were added from 0.05 to 1.0 mg/L, with a limit of detection (LOD) of 0.031 mg/L under the optimized conditions. Despite achieving high recovery rates in spiked samples of corn, rice, and feed, the proposed method for detecting OTA relies solely on MIPs for recognition [49]. While MIPs represent a significant advancement in recognition efficiency and accuracy, they are limited by their single recognition mechanism. Looking ahead, there is a potential trend toward developing hybrid synergistic identification systems that integrate two or more recognition elements.

2.4. Enzymes

As one of the most essential biological catalysts, enzymes can mediate biochemical reactions to improve efficiency [50,51]. Enzymes, which are protein-based compounds, selectively attach to substrates. For instance, Yin et al. reported the combination of enzymes and nanomaterials. The enzyme–nanomaterial composites were further used for the specific detection of *Cronobacter* spp. Later, using the same phenomena and UCNPs improved the fluorescence response during the detection of *C. sakazakii* [52]. These cationic UCNPs@MOF probes, the α-glucosidase enzyme, and para-nitrophenyl-α-D-glucopyranoside as an enzyme–substrate complex produced 4-nitrophenol as a quencher. A fluorescence and colorimetric dual-signal detection mode was developed to avoid false positives and improve the detection and precision of UCNP-based biosensors with enzymes [53]. For example, Ouyang et al. assembled a dual-signal composite detection system made of upconversion horseradish peroxidase–aptamer–magnetic nanoparticles to detect *S. aureus* in fresh meat. In this sensor, the aptamer complementary chain and horseradish peroxidase were tailored on the surface of the UCNPs, and the additions of *S. aureus* cells restored the supernatant's fluorescence intensity and absorbance values. The optimized reaction shown a strong linear relationship between fluorescence intensity and absorbance with

a logarithmic *S. aureus* concentration in the range of 56–5.6 × 10^6 cfu/mL. The LOD is 22 cfu/mL for fluorescence and 20 cfu/mL for colorimetry [54]. While enzymes are employed in UCNP-based biosensors, it is essential to note that challenges persist throughout the biosensor development process. These challenges primarily revolve around stability and diversity.

Table 1. Comprehensive overview of recognition elements utilized in UCNP-based biosensors.

Recognition Elements	UCNPs	Principle	Matrix	Advantages	Disadvantages	[a] Ref.
Antibodies	20% La^{3+}—doped $NaYF_4$: Yb, Er	FRET	Maize and wheat	Their high specificity gives UCNPs great selectivity. ICA has the advantages of simpler operation, faster detection, and easier result judgment.	Aside from being expensive, they may cause false positives due to cross-reactivity with highly homologous proteins.	[31]
	30% La^{3+}—doped $NaYF_4$: Yb, Er	FRET	Maize			[32]
	$NaYF_4$:Yb, Er and $NaYF_4$:Yb, Tm	FRET	Meat and milk			[35]
Aptamers	Mn^{2+}—doped $NaYF_4$:Yb, Tm	LRET	Milk	With lower storage conditions, it has the ability to specifically bind to targets from nanomolar to picomolar concentrations and can be prepared on a scale in a short time.	It has restrictions that prevent it from being widely applied due to the difficulties of binding to certain proteins.	[40]
	$NaYF_4$: Yb, Er	FRET	Maize			[10]
	$NaYF_4$: Yb, Er	FRET	Bottled water, milk, green tea powder, and fish			[42]
Molecularly imprinted polymers	$NaYF_4$: Yb, Er	FRET	Corn, rice, and feed	They can be applied widely due to their relatively controlled process, higher stability, and reusability.	They are not suitable for large-scale applications owing to the complicated preparation progress and the difficulty in choosing an appropriate template.	[46]
Enzymes	$NaYF_4$: Yb, Er	FRET	Tap water, infant formula powder, and goat milk powder	In addition to having a high specificity, they have superiority in productivity to accelerate a process, catalytic activity independent of an environment, and reversibility to achieve dynamic regulation.	They are required for a strict environment and matrix because of their high sensitivity for temperature and pH and high specificity.	[52]
	$NaYF_4$: Yb, Er	MNPs	Pork and beef			[54]

[a] Ref.: References.

3. Strategies of UCNP-Based Biosensors

As mentioned earlier, UCNPs play a crucial role in biosensors, particularly in converting target inputs into luminescence signaling responses. UCNP-based biosensors use chemical or biorecognition components to achieve this, and the reaction of these recognition elements to UCNPs is how pathogenic bacteria and their metabolites are detected. Common strategies for constructing UCNP-based detection systems include fluorescence resonance energy transfer (FRET), the inner filter effect (IFE), magnetic separation techniques, and other methods illustrated in Figure 4. The advantages and limitations of these approaches are summarized in Table 2.

3.1. Fluorescence Resonance Energy Transfer

FRET is the extensively applied approach for the development of UCNP-based biosensors. Forster proposed this in 1948 and explained the energy transfer phenomena of excited states. The phenomena state the energy transfer process from an energized donor particle to a receptor particle that absorbs light. Due to their excellent fluorescence attributes, UCNPs are often utilized as excellent energy donors. The spectral overlapping of emission and absorption spectra of the donor and acceptors and the distance among them determine the energy transfer efficiency. It has been documented that FRET only occurs at relatively short distances between the donor and the acceptor, around 10 nanometers, because the energy transfer occurs via resonant coupling through the donor–acceptor dipoles [55].

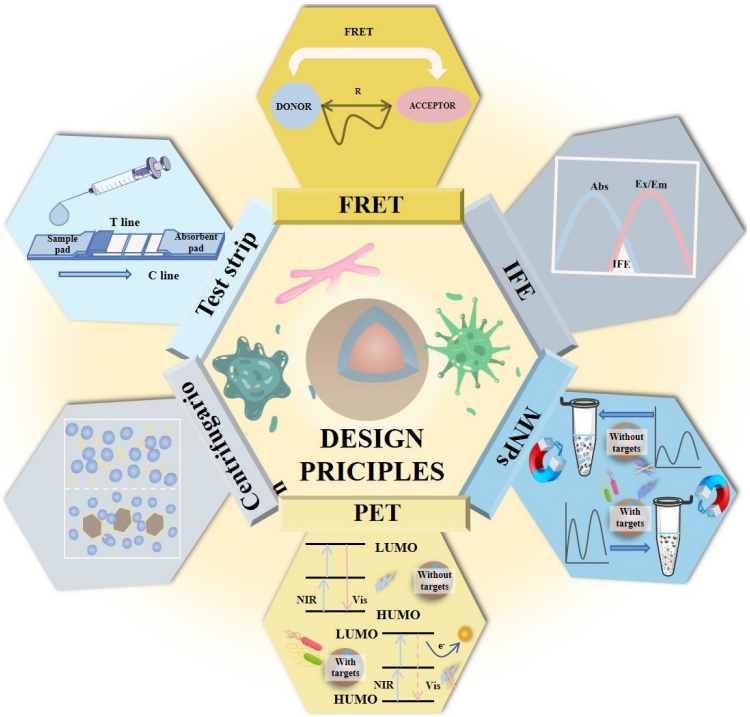


Figure 4. The design principles for constructing UCNP-based biosensors, including FRET, IFE, MNPs, PET, centrifugation, and test strips.

For instance, Jin et al. developed a FRET-based fluorescence biosensor for the rapid detection of *E. coli* ATCC 8739 in food samples, achieving results within 20 min. The sensor utilized gold nanoparticles (GNPs) linked to aptamers as the energy acceptor and UCNPs conjugated with complementary DNA (cDNA) as the donor. In the absence of the target, fluorescence was quenched, but upon the addition of the target, fluorescence was restored [56]. Similarly, Wang et al. introduced an innovative UCNP-based FRET aptasensor for the precise detection of aflatoxin B_1 (AFB_1) in peanut samples using UCNPs and aptamers as the luminescent donor and GNPs as the energy acceptor. Without AFB_1, the UCNPs and aptamers formed coordination bonds with GNPs due to nitrogen and gold atom interactions, which suppressed the UCNP–aptamer luminescence. Conversely, in the presence of AFB_1, UCNPs and aptamers bind specifically to AFB_1, releasing the GNPs from the UCNP–aptamer complexes [57]. Hence, it can be concluded that the FRET principle can help to create more sensitive detection systems using UCNPs for the identification of pathogens and their byproducts. Future research should focus on creating more precise recognition elements that maintain the proper distance for implementation. Additionally, an acceptor with greater spectral overlap and quenching efficiency would significantly improve the sensitivity of FRET within UCNP-based biosensors.

3.2. Inner Filter Effect

Besides the FRET, IFE is also one of the leading design principles for upconverting detection due to its advantages of being nonradiative, direct, and sensitive [58]. The IFE can occur when the absorbers absorb fluorophores' excitation and emission light [59]. In UCNP-based biosensors, the IFE offers greater flexibility than FRET since it is not dependent on the distance between the donor and the acceptor. The intensity of the IFE is determined by the overlap between the absorber's absorption spectrum and the fluorophore's fluorescence excitation and emission spectrum. When the target is present, changes in the acceptor's absorption band can modulate the emission of the UCNPs. Thus, IFE has emerged as a key principle in the detection of bacteria using UCNPs [41]. For instance, Wu et al. reported the

use of platinum-coated gold nanorods (AuNRs@Pt) combined with UCNPs to rapidly and accurately detect staphylococcal enterotoxin B (SEB), achieving a detection limit as low as 0.9 pg/mL, significantly lower than existing methods [60]. Similarly, Li et al. developed a UCNP-based biosensor with dual recognition capabilities for detecting *L. monocytogenes* in ham samples [61]. The upconversion fluorescence response was enhanced through the inner filter effect (IFE) between the colorful products generated via the horseradish peroxidase-3,3′,5,5′-Tetramethylbenzidine (HRP-TMB) reaction and the UCNPs. Remarkably, this method attained an impressively lower limit of detection of 2.8×10^2 cfu/mL. So, developing UCNP-based biosensors using IFE has a broad scope of applications. However, in the practical application process, IFE is considered as one of the leading causes of errors. Appropriate experimental design and new data analysis methods can minimize the adverse effects of the IFE.

3.3. Magnetic Separation Technique

In the 1950s, Neel made groundbreaking contributions to the study of magnetic behavior in magnetic nanoparticles (MNPs), laying the foundation for subsequent advancements. These MNPs have continued to captivate researchers due to their remarkable characteristics, such as small size effects, quantum size effects, and exceptional superparamagnetism [62,63]. These magnetic properties cause electrons to align in a specific manner when subjected to a magnetic field.

Unlike fluorescence resonance energy transfer (FRET) and the inner filter effect (IFE), magnetic separation offers the advantage of better preserving the optical properties of UCNPs. For example, Hu et al. fabricated oil-phase core–shell $NaYF_4$: Yb^{3+}, Tm^{3+} (20%/2%) @$NaYF_4$: Yb^{3+}, and Er^{3+} (x%/2%) (x = 20, 30, 50, 70, and 90) nanocrystals by varying Yb^{3+} concentrations. Through antigen–antibody recognition, sandwich complexes composed of an MNP, a bacterium, and UCNPs were formed. These complexes exhibited luminescence with varying red-to-green (R/G) ratios. This innovative approach enabled the identification and quantitative detection of five types of foodborne pathogens: *E. coli*, *S. paratyphi B*, *S. enteritidis*, *S. paratyphi C*, and *S. choleraesuis*. Detection was achieved by analyzing the R/G ratios and the intensity of green photoluminescence at 980 nm, ensuring accurate and reliable results [64,65]. For example, Chen et al. fabricated aptasensors based on MNPs@GO with UCNPs to detect *S. aureus*. When *S. aureus* is not present, MNPs@GO remain separate, and the upconversion fluorescence peak intensity does not change. For the availability of targets, MNP@GO complexes separate, isolating only the MNPs magnetically. This separation and reduction in fluorescence intensity from the apt-UCNP donor to the graphene oxide (GO) acceptor is based on the principle of FRET. To improve UCNP-based detection, [66] develop a rapid and cost-effective method for bacterial enrichment and purification. Additionally, a critical trend in food safety involves constructing multifunctional nanomaterials capable of simultaneously capturing and controlling pathogenic bacteria.

3.4. Others

In addition to these three principles, others are also used to detect food contaminants. These include photo-induced electron transfer (PET), centrifugation, and test strips. PET is a unique quenching mechanism in UCNP-based sensing systems consisting of a donor, an acceptor (fluorophore), and a bridge [67]. When the donor's highest occupied molecular orbital (HOMO) energy level is situated between the fluorophore's HOMO and lowest unoccupied molecular orbital (LUMO), intramolecular electron transfer from the electron donor to a neighboring acceptor takes place, producing the PET effect [68]. The absorption spectrum of the acceptor and the emission spectra of the donor do not overlap in the PET process, in contrast to energy transfer. There are some reports about UCNP-based

biosensors that help to guide the detection of pathogenic bacteria. For instance, Ouyang et al. developed mesoporous silica-modified upconversion nanoparticles (UCNPs-mSiO_2) for the ultra-sensitive detection of *S. aureus*. The mesoporous silica (MS) provided molecular channels and binding sites for Fe^{2+} ions. Upon forming the target–aptamer complex, Fe^{2+} was released from the mesopores and oxidized to Fe^{3+} in the presence of hydrogen peroxide (H_2O_2). The Fe^{3+} subsequently bound to the UCNPs, resulting in fluorescence quenching [69].

Centrifugation is also widely used to detect bacteria and their metabolites. The fluorescence intensity in the supernatant varies as the results of gathering the UCNP-bound target at the bottom due to the external centrifugal force. This approach is usually used to detect bacteria because it is heavier than nanoparticles. For instance, Li et al. constructed a fluorescence-based aptasensor for the detection of *S. aureus* [39]. In this sensor, *S. aureus* binds to core/shell upconversion nanoparticles (CS-UCNPs), allowing bacteria to be easily separated from the detection system through low-speed centrifugation. A UCNP–antibody–bacterium complex was formed to detect *E. coli* in milk following incubation and centrifugation. Following the optimization of centrifugation settings, this biosensor aimed to enhance the isolation of the complexes while preserving the integrity of the UCNP–antibody probes. The fluorescence intensity of the supernatant is directly correlated with the concentration of *E. coli*, reaching its maximum at 657 nm in the absence of targets [70]. In another study, based on the dual-color UCNPs, *E. coli* and *S. aureus* were detected simultaneously via centrifugation. While centrifugation-based UCNP sensing is fast and sensitive, its application remains limited to bacterial monitoring [35].

Test strips are recognized as compact, portable devices designed for the immediate and on-site swift identification of foodborne bacteria. Owing to their distinctive benefits, like ease of use, speed, affordability, and straightforward operation, test strips equipped with UCNPs are becoming a favored point-of-care testing tool in quick detection systems [34,71,72]. Test strip-based and UCNP-based biosensors use capillary force between paper fibers for on-chip analysis rather than pump-driven or electrically driven force [73]. Numerous efforts have been made to detect pathogens using single-test-strip-based UCNPs. Furthermore, Wu et al. developed an aptamer-based test strip for detecting OTA using $NaYF_4$: Yb, Er. Furthermore, to improve analytical performance, further investigations related to the optical properties of UCNPs, properties of the UCNP-apt complex, and the movement rate of UCNP-apt on the nitrocellulose membranes are required [74].

Table 2. Fundamental principles for UCNPs' detection of bacteria and their metabolites.

Design Principles	UCNPs	Recognition Elements	Matrix	Strengths	Weaknesses	[a] Ref.
Fluorescence resonance energy transfer	$NaYF_4$: Yb, Er	Apt	Tap/pond water and milk	It can be applied in a variety of fields with non-destructive, highly sensitive, real-time monitoring.	It is subjected to many factors, including the environment, a limited measuring distance, and spectra overlap.	[56]
	$NaYF_4$: Yb, Er	Apt	Peanut			[57]
Inner filter effect	$NaYF_4$: Yb, Er	Apt	Milk	It is not dictated by the donor–acceptor distance and cannot change the lifetime of UCNPs.	It is considered to be one of the main causes of error due to the complexity of data interpretation. In addition, it requires some organic molecules with toxicity as recognition elements.	[60]
	$NaYF_4$: Yb, Er	MNPs and Apt	Ham			[61]
Magnetic separation technique	$NaYF_4$: Yb, Tm	mAb	-	As a potential adsorbent, it can shorten the course of pro-processing, reduce background interference effectively, and preserve the optical properties of UCNPs via superparamagnetism, surface reactivity, and good chemical stability.	It restrict the number of sample which may require more processing time and resources for high-throughput applications. In addition, its stability is not very good.	[64]
	$NaYF_4$: Yb, Er	Apt	Chicken			[66]

Table 2. *Cont.*

Design Principles	UCNPs	Recognition Elements	Matrix	Strengths	Weaknesses	[a] Ref.
Photoinduced electron transfer	$NaYF_4$: Yb, Er	Apt	Pork and beef	It has a high selectivity because it usually occurs between specific molecules or between molecules and surfaces. In addition, it can improve the sensitivity, which causes a significant weakening or complete disappearance of the fluorescence signal	It is limited by its structure and may not be suitable for some samples or applications. And its rate and efficiency are affected by a variety of factors.	[69]
Centrifugation	$NaYF_4$: Yb, Tm@$NaYF_4$	Apt	Milk	With a lower storage condition, it has the ability to specifically bind to targets from nanomolar to picomolar concentrations and can be prepared on a scale in a short amount of time.	It has restrictions that prevent it from being widely applied due to the difficulties of binding to certain proteins.	[39]
	$NaYF_4$: Yb, Er	Abs	Meat and milk			[70]
	$NaYF_4$: Yb, Er and $NaYF_4$: Yb, Tm	Abs	Pork and milk			[35]
Test strips	$NaYF_4$: Yb, Er	Apt	Beer and wheat	They can be applied widely due to their relatively controlled process, higher stability, and reusability.	They are not suitable for large-scale applications owing to the complicated preparation progress and the difficulty in choosing an appropriate template.	[34]

[a] Ref.: references.

4. Innovation in Bacterial Sensing Using UCNP-Based Biosensors

Recently, UCNP-based biosensors have become indispensable tools for analyzing foodborne bacteria and their metabolites. Through specific biorecognition reactions, upconversion fluorescence can be modulated to detect pathogenic bacteria (*E. coli*, *L. monocytogenes*, *S. aureus*, and *Salmonella*). These UCNP-based biosensors for detecting pathogenic bacteria in food are listed in Figure S1 and Table S1.

4.1. Escherichia coli

Escherichia coli, commonly known as *E. coli*, has consistently threatened food safety and public health, drawing significant concern due to its potential to cause widespread harm. The major sources of *E. coli* contamination typically include unpasteurized milk, beef, green leafy vegetables, water, and various raw foods. The primary transmission route is fecal–oral, highlighting the importance of proper food handling, hygiene practices, and early detection [75,76]. *E. coli* contamination often results in severe bacterial infections and disease outbreaks, including urinary tract infections, kidney failure, meningitis, anemia, and hemorrhagic diarrhea [77]. It is essential to prioritize early spotting and subsequent treatment to mitigate health risks and complications. Several fluorescence sensors were reported for the early detection of *E. coli*. For instance, Pan et al. developed an antibody-based sensor for detecting *E. coli*, utilizing UCNPs as fluorescence probes. Changes in fluorescence signals were used to quantify concentrations ranging from 42 to 42 $\times$ 10^6 cfu/mL (R^2 = 0.9802) with a limit of detection (LOD) of 10 CFU/mL. In addition to antibodies, magnetic nanoparticles (MNPs) were also employed to construct UCNP-based biosensors for *E. coli* detection in pork [70]. Although with *S. aureus* and *S. typhimurium*, this system still has recognition specificity issues [32,78,79]. As illustrated in Figure S1A, a dual-mode biosensor combining colorimetric and fluorescence detection was developed using alendronic acid (ADA)-coated UCNPs and Nile Blue (NB) for the detection of *E. coli*. This sensor combined PCR and IFE to achieve excellent sensitivity, eliminating the separation steps, the duration of the detection process (1 h), and other stringent distance requirements [80]. Usually, *E. coli* exists in a complex matrix, which may contain various substances, resulting in the reduced specificity and selectivity of UCNPs and increasing the risk of false positives or negatives. In addition, the concentrations of *E. coli* have a wide range, while the sensitivity of UCNPs

may be limited via detection. Thus, future research must optimize experimental conditions, minimize interference, and broaden the measurement range.

4.2. Listeria monocytogenes

Listeria monocytogenes (*L. monocytogenes*), a foodborne bacterium, is commonly present in milk, meat, aquatic products, ready-to-eat meals, and frozen and chilled foods. This bacterium exhibits resilience to lower temperatures, acidity, and higher salt concentrations, and it can penetrate the food chain via contaminated food and infected animals [59]. That is why the improvement of UCNP-based detection probes has gained attention for the quick and reliable detection of *L. monocytogenes* to protect people's well-being and facilitate the food industry. For example, Yin et al. introduced three chemicals to modify UCNP-based probes such as the positively charged imidazole ionic liquid group, negatively charged phenylboronic acid, and phosphate groups to increase the fluorescence response toward bacteria [81]. In addition, Liu et al. reported a sensor that consists of three UCNPs which successfully distinguish seven bacteria, including *L. monocytogenes*, in different food samples. A fluorescence aptasensor was developed to detect *L. monocytogenes* using aptamer-functionalized UCNPs and MNPs. The sensor included concentration probes and signal probes that generated a robust fluorescence signal, as presented in Figure S1B. A strong correlation was observed between the fluorescence intensity and the concentration of *L. monocytogenes* in the range of 68 to 68 $\times$ 10^6 cfu/mL [82]. The remarkable thing is that the growth rate of *L. monocytogenes* is relatively slow, so real-time monitoring-based UCNP sensors were used. Hence, searching for suitable enrichment and purification methods is necessary to detect *L. monocytogenes* quickly and sensitively.

4.3. Staphylococcus aureus

Staphylococcus aureus (*S. aureus*) is a well-known foodborne bacterium that has garnered significant attention due to its pathogenicity. It is primarily transmitted to humans through the consumption of contaminated high-protein foods, such as meat, fish, eggs, and milk, which are essential components of the daily human diet [66,83]. Notably, *S. aureus* can cause a range of illnesses, from mild skin and soft tissue infections (e.g., boils and impetigo) to severe diseases, including sepsis, pneumonia, and endocarditis [69,84]. Consequently, the early detection of *S. aureus* is critical for mitigating the risks of foodborne outbreaks and safeguarding public health.

To address this need, various UCNP-based biosensors have been developed due to their superior performance. For instance, Chen et al. constructed an aptasensor by integrating MNPs@GO and aptamer-functionalized UCNPs for *S. aureus* detection. In this system, the introduction of the target caused a reduction in upconversion fluorescence intensity at 547 nm due to FRET phenomena, achieving a remarkably low detection limit of 13 cfu/mL [66]. Similarly, another study designed a CS-UCNP-based aptasensor for detecting *S. aureus*, which provided a specific fluorescence signal and high sensitivity. The substantial size difference between the nanoparticles and *S. aureus* (approximately 30-fold) allowed for easy separation via centrifugation, eliminating the need for complex FRET mechanisms [39].

Furthermore, Ouyang and her team developed a colorimetric–fluorescent dual-mode nanoprobe with the assistance of HRP. This system utilized apt-MNPs as signal capture probes and HRP-UCNPs-cDNA as colorimetric signal probes, enabling the rapid detection of *S. aureus* in meat samples, as illustrated in Figure S1C [54]. Notably, most existing studies on UCNP-based biosensors focus on detecting individual *S. aureus* strains. However, an emerging trend involves designing sensors capable of simultaneously detecting multiple bacteria to enhance their efficiency and their broaden their application potential.

4.4. Salmonella

Salmonella, a notorious foodborne pathogen, is known for its ability to specifically target humans as hosts [85]. It can cause a range of diseases, primarily through intestinal infection. This bacterium is adept at invading the human gastrointestinal tract, leading to conditions ranging from mild gastroenteritis to more severe illnesses, potentially resulting in significant health complications if not promptly treated [41]. In past decades, *Salmonella* has been responsible for nearly 100 million cases of foodborne illness, resulting in economic costs exceeding 365 million USD. According to the World Health Organization (WHO), *Salmonella* is a prevalent foodborne bacterium. Traditional detection methods, such as immunological assays and PCR techniques, are widely used [85]. However, these methods require extended detection times (4–6 h), are prone to false positives, and involve complex procedures. Consequently, developing highly sensitive and efficient detection methods, such as UCNP-based biosensors, is crucial for monitoring *Salmonella* contamination. For example, Chen et al. designed a FRET-based aptasensor for *Salmonella* detection. By measuring the energy transfer between ADA@UCNPs and AuNPs under optimal conditions, this sensor enabled the quantification of *Salmonella* concentrations across a wide range (from 1.16×10^2 to 1.16×10^7 cfu/mL) with a remarkably low limit of detection (LOD) of 36 cfu/mL [50].

As displayed in Figure S1D, this group also constructed a biosensor to detect *Salmonella* sensitively with UCNPs as signal probes and MNPs as a capture probe based on the ADA@UCNPs and mitoxantrone dihydrochloride (MTX). The IFE improves sensitivity based on MTX's capability to overlap the upconversion fluorescence emission spectrum, reducing UCF intensity [86]. Despite detecting *Salmonella* based on UCNP sensing, which holds great vitality and tremendous growth potential, essential problems, including stability during storage and the cost of production, still need to be addressed.

5. Innovation in Metabolite Analysis Using UCNP-Based Biosensors

Pathogenic bacteria are not only harmful but also produce toxic metabolites that are challenging to eliminate. Similarly, filamentous fungi are well known for generating toxic secondary metabolites called "mycotoxins", which pose severe risks to human and animal health. Mycotoxins such as aflatoxin B_1, ochratoxin A, fumonisin B_1, and deoxynivalenol have profound toxicological and economic impacts. To address these challenges, various biosensors based on UCNPs have been developed to detect these hazardous metabolites, as depicted in Figure S2 and summarized in Table S1.

5.1. Aflatoxins B_1

Aflatoxins are a class of toxic substances that can have enormous health consequences for humans and animals. These hazardous chemical compounds are produced by fungi, particularly *Aspergillus flavus* and *Aspergillus parasiticus*, under favorable conditions and the improper storage of grains and other food commodities [87–91]. According to the International Agency for Research on Cancer (IARC, 2002), aflatoxin B_1 (AFB_1) is classified as a carcinogen. Given its mutagenic, teratogenic, carcinogenic, and immunosuppressive effects, the rapid detection of AFB_1 is technologically critical [32,92]. Owing to their exceptional optical properties, UCNP-based sensors have proven highly effective for detecting aflatoxins in food samples. For instance, in 2016, our earlier work developed a novel fluorescence probe for detecting AFB_1. This was achieved by crosslinking UCNPs and immunoproteins with antigen-modified MNPs as immunosensing probes, while antibody-functionalized $NaYF_4$ UCNPs acted as color signal probes [93].

Additionally, a sensitive aptasensor for the rapid detection of AFB_1 was fabricated using a single-particle detection assay to count UCNP–aptamer complexes, as shown in

Figure S2A. This sensor demonstrated a linear detection range from 3.13 to 125.00 ng/mL under optimal conditions, with a lower detection limit of 0.17 ng/mL [57]. Moreover, the integration of fluorescein isothiocyanate, a pH-sensitive dye, allowed for the development of a microenvironment-responsive UCNP immunosensor based on Förster resonance energy transfer (FRET), achieving a remarkable quenching efficiency of 95% (compared to the usual <80%). Simultaneously, the fluorescence signal was amplified using trace AFB_1-induced acetylcholine esterase-coated UCNPs, resulting in an exceptionally low limit of detection (LOD) of 0.003 nM [94]. Given the significant toxicity of AFB_1, further efforts should focus on optimizing UCNP-based detection systems for on-site applications. Additionally, designing user-friendly operational interfaces to reduce the complexity of procedures remains a key area for investigation.

5.2. Ochratoxin A

Aspergillus and *Penicillium* are recognized as the primary producers of ochratoxins, with Ochratoxin A (OTA) being the most prevalent [48,95–98]. OTA is found in various food commodities, including cereals, wheat, and barley. The consumption of contaminated food can lead to nephrotoxic, immune-toxic, teratogenic, and carcinogenic effects in humans. Consequently, the International Agency for Research on Cancer (IARC) has classified OTA as a Group 2B carcinogen due to its significant risk to human health and potential impact on the social economy [99–104]. To enhance OTA monitoring accuracy and ensure better food safety, numerous UCNP-based sensors have been developed and applied. For instance, hexagonal CS-UCNP-based ultrasensitive biosensors have demonstrated a strong linear correlation between luminescence intensity and OTA concentration, ranging from 0.001 ng/mL to 250 ng/mL, with an impressive limit of detection (LOD) of 0.001 ng/mL [105]. Moreover, Jin et al. introduced an innovative immunoassay using blue-green-red multicolor UCNPs to detect cereal mycotoxins, including OTA. As illustrated in Figure S2B, anti-OTA antibodies were conjugated with UCNPs as signal probes, while OTA-coating antigens were attached to magnetic polystyrene microspheres as capture probes. This approach enabled the biosensor to achieve superior sensitivity (LOD = 5.6×10^{-4} ng/mL) and a broader detection range (0.032 to 200 ng/mL) [106]. In addition to these advancements, numerous UCNP-based assays have been designed for the detection of various mycotoxins, including the simultaneous identification of OTA. For future improvements, exploring enhancements in assay sensitivity, specificity, and multiplexing capabilities may be beneficial to broaden the range of detectable mycotoxins and improve overall assay performance.

5.3. Fumonisin B_1

Besides the OTA mentioned above, fumonisin B_1 (FB_1) has also been categorized as a carcinogen in group 2B. As a well-known mycotoxin in corn, FB_1 is primarily produced by *Fusarium moniliforme* and *Fusarium proliferatum* [107–109]. Considering its toxicity and prevalence, various traditional detection assays have been reported to detect FB_1 rapidly. However, they are inaccessible to all because they are only present in sophisticated laboratories and are not available for rapid testing. Fortunately, UCNP-based sensing enabled FB_1 detection in food samples without any background interference, and several detection strategies were adopted to fabricate UCNP-based biosensors for FB_1. For instance, Wu et al. developed an aptasensor based on FRET between $NaYF_4$: Yb, Ho UCNPs and AuNPs to detect FB_1 in corn samples. This system achieved a detection range of 0.01 to 100 ng/mL with a detection limit (LOD) of 0.01 ng/mL, as illustrated in Figure S2C [107]. In a separate study, an aptasensor employing the IFE strategy was designed for the rapid detection of two types of mycotoxins. This detection system utilized 65 nm AuNRs, 20 nm UCNPs, fluorescent dyes, and DNA sequences. The study demonstrated that fluorescence intensity

correlated with FB_1 concentration within the range of 0.01–100 µg/L, achieving an R^2 value of 0.986 and a detection limit of 0.003 ng/L [109].

5.4. Deoxynivalenol

Deoxynivalenol (DON), also known as vomitoxin, is a highly potent mycotoxin belonging to the trichothecene subgroup B. It is primarily produced by the Fusarium species and represents a major threat to both human and animal health [110,111]. DON is highly toxic and can cause a variety of adverse effects like acute feed refusal, weight loss, cardiac issues, developmental problems, immune system issues, and cellular death [112]. It is a water-soluble toxin that is likely to spread through water and soil and contaminate foodstuff, affecting human health, livestock, and poultry throughout the food chain. Many studies have been conducted to design UCNP-based biosensors for detecting DON to prevent its destructive impact on agriculture and society [113,114]. For example, Lin et al. developed a CRISPR-Cas12a-mediated aptasensor based on the LRET phenomenon to detect DON in water and corn flour samples. As illustrated in Figure S2D, the biosensor employed ssDNA and UCNPs as luminescent markers and GNP-decorated Ti_3C_2Tx MXene nanosheets (MXene-Au) as quenchers. The fluorescence response variation enabled the quantification of target concentrations within a linear dynamic range of 1–500 ng/mL, with a detection limit (LOD) of 0.64 ng/mL [115]. For the simultaneous detection of AFB_1 and DON, a fluorescence probe was developed by integrating UCNPs via magnetism-induced separation. This design facilitated the specific formation of UCNP–antibody–antigen–MNP and UCNP–antibody–target complexes [116]. Additionally, [28,117] developed a dICA where UCNPs were utilized as fluorescent tags and AuNPs as fluorescence quenchers. This method enabled the simultaneous detection of OTA and DON on two test lines by implementing a bidirectional T-line configuration.

6. UCNP-Based Biosensors for Point-of-Care Application

In the previous section, we discussed the construction and high performance of UCNP-based biosensors in detecting foodborne bacteria and their metabolites. However, pathogenic bacteria are pervasive, potentially contaminating every stage of the food supply chain, from production and packaging to transportation and sales. Given the limited availability of large instruments and skilled professionals in such situations, point-of-care technologies have been widely developed to bridge this gap. These include test strips, microfluidics, photoelectrochemistry, and smartphone-based systems. Figure 5 provides an overview of these technologies, while Table 3 presents illustrative examples for reference.

6.1. Portable Detection

6.1.1. Lateral Flow Assay-Based Detection

Lateral flow assays (LFAs), an improved dipstick assay, have been extensively explored owing to their lower cost, less time, simplicity, high sensitivity, and convenience. LFAs constructed with UCNPs have demonstrated their efficiency in detecting foodborne bacteria and metabolites. Typically, the structure of UCNP-based LFAs comprises four components: the sample pad, the conjugation pad, the detection pad, and the absorbent pad [118]. To achieve qualitative and quantitative analyses, the test (T) line and the control (C) line were designed on a detection pad [119]. Based on identifying antigens and antibodies, incorporating UCNPs in ICA is a suitable approach for developing an on-site detection system at a large scale. For example, a dual-channel ICA with IUCNPs was developed to detect AFB_1 and ZEN simultaneously within 10 min. Compared to conventional UCNPs, IUCNPs have a larger size, more regular shape and structure, and higher fluorescence intensity [32]. In addition, Chen et al. fabricated a dual-flux bidirectional single-line

labeling immunochromatographic assay to detect OTA and DON simultaneously on two test lines with UCNPs as a signal reporter. In the presence of targets, UCNPs emitted green fluorescence at 540 nm. And the C line was designed based on the red fluorescence (660 nm) of UCNPs [28].

However, the use of antibodies in real-time detection is less common due to the laborious, complex, and costly preparation for small molecules [120]. The aptamer is a better candidate due to its ease of synthesis, low cost, long shelf life, higher affinity, and specificity [99]. For example, Wu et al. established an aptamer-based test strip based on the UCNPs for quantitatively detecting ZEN with specificity and sensitivity. Figure 5A accurately depicts that the ZEN concentration can be further calculated with the help of an MZ-6000 colloid gold reading instrument to accurately determine the color intensity of T and C lines [34]. The concentration shows good linearity under the optimized conditions. While UCNPs and LFAs hold promise for qualitative bacteria and metabolite detection, their application is hindered by the requirement for peripheral devices to stimulate signals and interpret results, which need to be more cost-effective.

6.1.2. Microfluidic-Based Detection

Microfluidic devices, or "lab-on-a-chip", integrate all steps, including sample preparation, reaction, separation, and detection, into a single chip, leveraging their excellent attributes such as miniaturization, high throughput, low sample consumption, and cost-effectiveness [121–123]. Glass, polymers, thermoplastic, glass polymers, thermoplastic, and cloth are the various materials used to construct UCNP-based microfluidic devices. For example, Chen et al. fabricated a sensitive microfluidics platform with plastic (polymethyl methacrylate, PAMM) to detect four mycotoxins simultaneously. The developed assay detected the T-2 toxin, AFB_1, OTA, and ZEN within 30 min [124]. This biosensor is made of plastic, which leads to high expenses. However, external instruments (a laptop and a camera) are also required to control the flow. To solve this problem, UCNPs and paper-based microfluidic analytical devices (μPADs) with low-cost and self-powered fluidic transport were developed [125–128]. For instance, Lin et al. developed a paper-based microfluidic aptasensor that simultaneously detects ZEN and OTA. This sensor uses green UCNPs (GUCNPs) and blue UCNPs (BUCNPs) as fluorescence labels, while Cu-TCPP nanosheets act as fluorescence quenchers. By combining UCNPs with microfluidic technology, this sensor enables rapid pathogen detection, as illustrated in Figure 5B [129]. Therefore, it is highly probable that even small quantities of pathogenic microorganisms can be quickly and accurately analyzed and detected.

6.2. Peripheral Devices

6.2.1. Photoelectrochemistry-Based Detection

Photoelectrochemistry (PEC), integrated photochemical and electrochemical technologies, are sensitive analytical assays. Typically, most PEC systems use ultraviolet or visible light to excite the sample, which involves some inherent obstacles (e.g., causing severe interference and damage to biological systems) [130,131]. UCNPs are a new NIR response material that combines a host material with a luminescent center, which is used as a light source [29]. Due to its unique property of "light excitation, electrical detection", PEC sensors with UCNPs have the advantage of low background, device portability, and ease of operation, that is why it can be an alternative to POCT. When light is converted from NIR via UCNPs irradiating the photosensitive materials (molecule, ion, or semiconductor material), an electronic transition occurs inside the materials, producing photoelectron–hole pairs [132]. Subsequently, the photo-to-electricity signal conversion occurs under a specific condition. For instance, Zheng et al. constructed a near-infrared-mediated photoelectro-

chemical immunosorbent assay (cNIR-PECIA) based on UCNPs, three-dimensional (3D) hierarchical WO_3 flower (FL-WO_3), and chitosan (CS) for the portable detection of okadaic acid (OA), which is a component of diarrhetic shellfish poison (DSP). FL-WO_3 is a photosensitive material with special light-absorbing properties and can absorb the maximum light from UCNPs. Then, the excitation of the electron–hole pair and the generation of photocurrent are achieved through the emission from UCNPs with the absorption [130].

Yin et al. fabricated a 3D paper-based NIRPEC for the on-site detection of *E. coli* O157:H7 with core–shell structures UCNPs@SiO_2@Ag and carbon self-doped graphitic carbon nitride C-g-C_3N_4. Figure 5C shows that, under 908 nm excitation, UCL was emitted by UCNPs, and then photoelectron–hole pairs of C-g-C_3N_4 were separated to generate a photocurrent. Silver nanoparticles were critical in enhancing the UCL and promoting the separation of electron–hole pairs in this system. Integrated sensing platforms that combine UCNPs and PET are vital for developing and applying POCT. However, the limitation of these PEC biosensors, which rely on UCNPs, is that they can only be detected in vitro. Therefore, developing UCNP-PEC sensors suitable for in vivo detection should be considered for future applications [133].

6.2.2. Smartphone-Based Detection

With the miniaturization, low cost, and ubiquity of smartphones, UCNP biosensors with smartphones have become a potential option instead of traditional laboratories in testing foodborne bacteria and their metabolites owing to high visibility, availability, and convenience [23,134]. In addition, a smartphone can eliminate the expensive cost of signal readers [76], integrate data recording and analysis, and achieve remote monitoring with the support of 5G. According to the Lambert–Beer law, UCNP sensing constructed with a smartphone is qualified to measure the concentration of the analyte by distinguishing differences in colors via a camera. For example, Lin et al. reported the installation of a color recognition app and a high-resolution camera and successfully merged a smartphone into a microfluidic aptasensor based on UCNPs to quantitatively monitor the concentration of ZEN and OTA by examining the "G & B" channel values from the green and blue images that correspond to the fluorescence intensity, which is proportional to the concentration at 808 nm. The camera uses a NIR shortwave pass filter to prevent interference from the excitation light in the captured image [129]. To address the challenges posed by external lasers, Gong et al. developed a handheld UCNP-LFA biosensor, a UCNP-LFA reader compatible with smartphones, and a custom-designed app analyzer (Figure 5D). An app makes the difference between the optical density of the test line and the background to obtain on-site and quantitative data on the target, including OTA. Furthermore, this platform is miniature compared with the existing equipment that has a dimension of 24.0 cm × 9.4 cm × 5.4 cm (L × W × H) and a weight of 0.9 kg [135]. In the future, smartphone-based detection using UCNPs could be developed to detect multiple bacteria and enhance efficiency simultaneously. Additionally, using 3D-printed materials represents a forward-looking approach that could reduce material consumption.

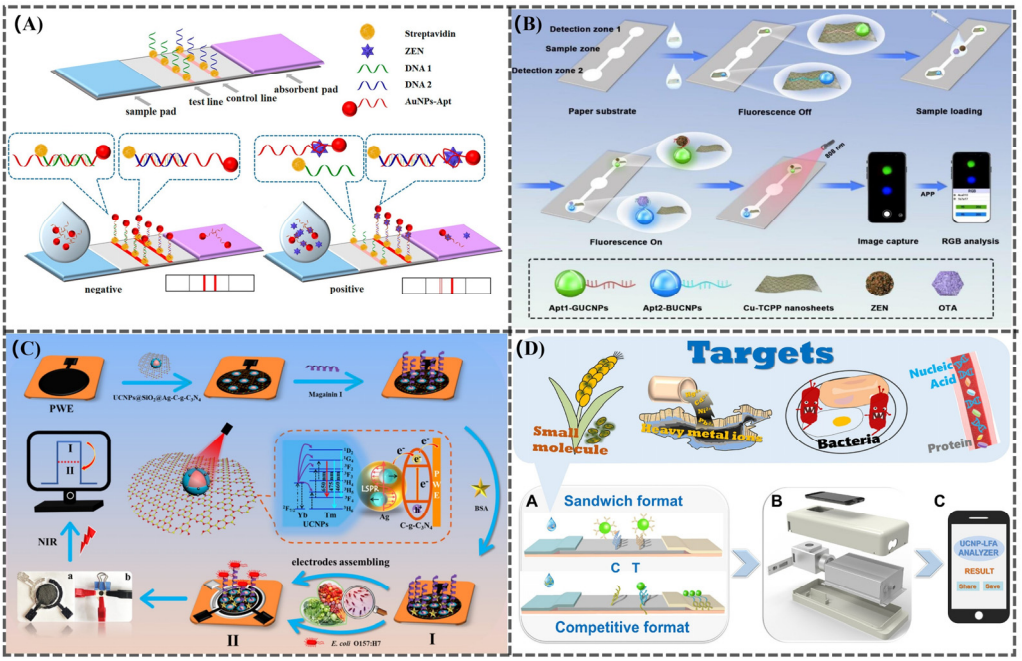


Figure 5. Schematic illustration of (**A**) an aptamer-based LFA based on UCNPs for the quantitative detection of ZEN [34]; (**B**) an aptamer-based test strip based on the UCNPs for quantitatively detecting ZEN [129]; (**C**) a cNIR-PECIA based on UCNPs for the portable detection of OA [133]; (**D**) a handheld UCNP-LFA biosensor with the assistance of a smartphone [135].

Table 3. Deployment of a UCNP-based biosensor integrated with POCT.

POCT Devices	Analyte(s)	UCNPs	Recognition Elements	Principle	[a] LOD	[b] LR	R^2	Recoveries	Samples	[c] Ref.
Lateral flow assays	AFB_1	30% Lu^{3+}—doped $NaYF_4$: Yb, Er	Abs	FRET	0.025 ng/mL	0.025 to 25 ng/mL	0.9931	-	Corn	[32]
Lateral flow assays	ZEN	30% Lu^{3+}—doped $NaYF_4$: Yb, Er	Abs	FRET	0.1 ng/mL	0.1 to 50 ng/mL	0.9982	-	Corn	[32]
Lateral flow assays	OTA	$NaErF_4$: Yb, Tm@$NaYF_4$: Yb@$NaNdF_4$: Yb	Abs	LRET	2.30 µg/kg	-	0.94	86.2 to 98.3%	Wheat	[28]
Lateral flow assays	DON	$NaErF_4$: Yb, Tm@$NaYF_4$: Yb@$NaNdF_4$: Yb	Abs	LRET	2.33 µg/kg	-	0.94	87.9 to 99.6%	Corn	[28]
Lateral flow assays	OTA	$NaYF_4$: Yb, Er	Apt	FRET	1.86 ng/mL	5 to 100 ng/mL	0,9955	95.2 to 115.6%	Beer	[74]
Microfluidic	T-2 toxin	$NaYF_4$: Yb, Er	Abs	FRET	0.12 ng/mL	0.28–3.91 ng/mL	0.9891	94.2 to 103% and 92 to 93.3%	Drinking water and corn	[124]
Microfluidic	AFB_1	$NaYF_4$: Yb, Er	Abs	FRET	0.03 ng/mL	0.12–7.19 ng/mL	0.9990	93.5 to 108% and 90.7 to 104%	Drinking water and corn	[124]
Microfluidic	OTA	$NaYF_4$: Yb, Er	Abs	FRET	1.24 ng/mL	2.32–19.37 ng/mL	0.9951	87.6 to 105% and 84 to 107.3%	Drinking water and corn	[124]
Microfluidic	ZEN	$NaYF_4$: Yb, Er	Abs	FRET	0.58 ng/mL	1.29–16.88 ng/mL	0.9956	107 to 108.1% and 86.7 to 109.5%	Drinking water and corn	[124]
Microfluidic	ZEN	$NaYF_4$: Yb, Er@$NaYF_4$: Yb, Nd and $NaYF_4$: Yb, Tm@$NaYF_4$: Yb, Nd	Apt	FRET	0.44 ng/mL	0.5–100 ng/mL	0.9980	94.5–103.7%	Corn flour	[129]
Microfluidic	OTA	$NaYF_4$: Yb, Er@$NaYF_4$: Yb, Nd and $NaYF_4$: Yb, Tm@$NaYF_4$: Yb, Nd	Apt	FRET	0.098 ng/mL	0.1–50 ng/mL	0.9862	92.2–106.8%	Corn flour	[129]
Photoelectrochemistry	DSP	$NaYF_4$: Yb, Tm	Abs	FRET	0.007 ng/mL	0.01–60 ng/mL	0.9907	96.2–102.5%	Shellfish	[29]
Photoelectrochemistry	*E. coli*	$NaYF_4$: Yb, Tm	Peptide	FRET	2 cfu/mL	5–5 × 10^6 cfu/mL	0.996	-	Pork, cabbage, and milk	[128]
Smartphone	ZEN	$NaYF_4$: Yb, Er@$NaYF_4$: Yb, Nd and $NaYF_4$: Yb, Tm@$NaYF_4$: Yb, Nd	Apt	FRET	0.44 ng/mL	0.5–100 ng/mL	0.9980	94.5–103.7%	Corn flour	[129]
Smartphone	OTA	$NaYF_4$: Yb/Er@$NaYF_4$	Abs	FRET	-	-	0.995	-	-	[135]

[a] LOD: lower of detection; [b] LR: linear range; [c] Ref.: references.

7. Conclusions and Future Perspectives

Foodborne bacteria are one of the leading causes of acute and chronic diseases. Therefore, it is imperative to detect and monitor them early to trace outbreaks and ensure consumer health and safety. In this context, UCNPs have emerged as a promising material widely used to observe pathogenic bacteria and their metabolites. Specifically, UCNPs offer numerous advantages, including substantial anti-Stokes shifts, low toxicity, enhanced light penetration, the absence of autofluorescence, narrow emission spectra, and a high signal-to-noise ratio. Consequently, this review provides a detailed overview of the recognition elements and design strategies employed in UCNP-based biosensors. Furthermore, the article highlights the use of these biosensors for detecting various bacteria and their metabolites. In addition, it explores the application of UCNP-based POCT as a portable and on-site platform for food safety analysis. Specifically, this review examines the use of UCNP-based POCT for detecting pathogenic bacteria and their metabolites, with a focus on lateral flow assays, microfluidics, photoelectrochemistry, and smartphone applications.

However, significant progress has been made in using UCNPs to improve biosensor systems for detecting food safety and quality. However, it is important to note that this field has not yet reached its full potential. Firstly, many platforms require complex pre-treatment steps to reduce the impact of diverse simple and complex matrices, which can increase operational complexity and time requirements. To streamline sample preparation processes and introduce advanced nanoprobes to reduce processing steps, simplified pre-treatment methods should be proposed to meet the future trend of real-time detection. Secondly, most UCNP-based biosensors have been tested on single-species bacteria, especially in POCT. However, this does not meet practical application requirements due to the co-existence of pathogenic bacteria and their synergistic and accumulative effects. The microplate-reading approach, the microzone paper method, and 3D PADs are well established in clinical analysis and could offer a promising solution in this context. By integrating multi-color and multi-channel emission strategies, this could provide a more robust platform for detecting a broader range of pathogens [136]. Low quantum efficiency is also a significant factor that hinders the advancement of UCNPs in bio-detection. This challenge can be overcome by considering the synergistic effects of particle size and probe density. Furthermore, it is crucial to account for the strong absorption effect of water in the NIR wavelength region, which can reduce the efficiency of UCNP-based detection [137]. Using higher-power NIR laser sources (up to 1W) and minimizing the water layer could significantly reduce this effect and improve performance. In addition, another factor limiting the full potential of UCNPs is particle size. Larger nanoparticles tend to have poor dispersibility, which negatively affects their response speed. By modifying the composition and structure of UCNPs, smaller and brighter nanoparticles can be fabricated, enhancing both stability and detection efficiency [138]. Failing to address these challenges could lead to more severe problems, resulting in diminished development prospects for UCNP-based biosensors.

The use of UCNPs in pathogen detection for POCT is becoming more portable, but that still needs to be addressed before commercialization. The first challenge is the cost. Although constructing UCNP-based biosensors for POCT is cheaper than traditional sensors, it must still be made more affordable to meet market requirements, especially in resource-limited areas. One way to do this is to find a more stable and inexpensive method for synthesizing and applying upconversion fluorescent materials. Breaking the sensor into separate modules also makes the maintenance and replacement of defective elements easier, which lowers the maintenance cost. Streamlining the sensor design can also reduce material costs and optimize production and maintenance costs. The second challenge is the susceptibility of point-of-care devices to environmental factors, which can compromise their accuracy and sensitivity. This can result in false positives and an inability to detect

low concentrations of pathogenic bacteria. Future designs should incorporate waterproof, dustproof, seismically robust packaging materials, environmental monitoring, automatic calibration, temperature control technologies, and circuits and signal processing devices with anti-interference capabilities to address these issues. These enhancements can protect the sensor's internal components from external environmental factors, detect environmental changes, and automatically adjust parameters across a broad temperature range. They can also reduce the impact of external electromagnetic interference on the equipment's performance. By addressing these challenges and adhering to international standards, UCNP-based POCT biosensors can be produced on a large scale and become a part of everyday life.

The abovementioned requirements must be met before introducing the sensors to the market. Currently, only a few biosensors using UCNPs for POCT are available for detecting pathogenic bacteria and their metabolites. By integrating with colorimetric assays or 3D paper-based devices, portability and versatility can be achieved. With advancements in recognition elements, nanomaterials, and sensing technology, there is great potential for developing UCNP- and biosensor-based POCT. These sensors are expected to play a critical role in detecting pathogenic bacteria and their metabolites and have a wide range of applications in the future.

Supplementary Materials: The following supporting information can be downloaded at https://www.mdpi.com/article/10.3390/chemosensors13020060/s1, Figure S1: The work principles of (A) a colorimetric and fluorescence dual-mode UCNP biosensor to detect *E.coli* [80]; (B) an aptasensor based on UCNPs and MNPs to detect *L. monocytogene* [82]; (C) a UCNP platform with apt-MNPs and HRP-UCNPs-cDNA [54]; (D) ultrasensitive detection for Salmonella using ADA@UCNPs and MTX [86]. Figure S2: Schematic illustration of (A) a single-particle AFB_1 detection by counting the number of UCNPs and aptamers [57]; (B) blue-green-red multi-color UCNPs to detect OTA, ZEN, and AFB_1 [106]; (C) FRET sensing based on UCNPs and AuNPs to detect FB_1 [107]; (D) a CRISPR-Cas12a-mediated UCNP biosensor based on the LRET principle to detect DON [115]. Table S1: Application paradigms for UCNP-based biosensors in pathogens and metabolites within food [39,50,54,57,70,75,80–82,86,93,94,105–107,110,115,116].

Author Contributions: H.L.: Conceptualization, investigation, writing—original draft, writing—review, and editing. Y.W.: Supervision, writing—review, and editing. M.S.: Writing—review, editing. W.S.: Writing—review, editing. Q.B.: Writing—review, editing. A.M.: Writing—review, editing. All authors have read and agreed to the published version of the manuscript.

Funding: This work has been financially supported by the National Key Research and Development Program of China (2023YFE0105500-3) and the National Foreign Experts Program (H20240213).

Conflicts of Interest: The authors declared that they have no conflicts of interest in this work.

References

1. Selva Sharma, A.; Marimuthu, M.; Varghese, A.W.; Wu, J.; Xu, J.; Xiaofeng, L.; Devaraj, S.; Lan, Y.; Li, H.; Chen, Q. A review of biomolecules conjugated lanthanide up-conversion nanoparticles-based fluorescence probes in food safety and quality monitoring applications. *Crit. Rev. Food Sci. Nutr.* **2024**, *64*, 6129–6159. [CrossRef] [PubMed]
2. Wang, J.; Chen, Q.; Belwal, T.; Lin, X.; Luo, Z. Insights into chemometric algorithms for quality attributes and hazards detection in foodstuffs using Raman/surface enhanced Raman spectroscopy. *Compr. Rev. Food Sci. Food Saf.* **2021**, *20*, 2476–2507. [CrossRef]
3. Shoaib, M.; Shehzad, A.; Raza, H.; Niazi, S.; Khan, I.M.; Akhtar, W.; Safdar, W.; Wang, Z. A comprehensive review on the prevalence, pathogenesis and detection of *Yersinia enterocolitica*. *RSC Adv.* **2019**, *9*, 41010–41021. [CrossRef] [PubMed]
4. Su, M.; Liu, F.; Luo, Z.; Wu, H.; Zhang, X.; Wang, D.; Zhu, Y.; Sun, Z.; Xu, W.; Miao, Y. The antibacterial activity and mechanism of chlorogenic acid against foodborne pathogen *Pseudomonas aeruginosa*. *Foodborne Pathog. Dis.* **2019**, *16*, 823–830. [CrossRef] [PubMed]

5. Yao, P.; Gao, Y.; Simal-Gandara, J.; Farag, M.A.; Chen, W.; Yao, D.; Delmas, D.; Chen, Z.; Liu, K.; Hu, H.; et al. Litchi (*Litchi chinensis* Sonn.): A comprehensive review of phytochemistry, medicinal properties, and product development. *Food Funct.* **2021**, *12*, 9527–9548. [CrossRef] [PubMed]
6. Ismail, A.; Naeem, I.; Gong, Y.Y.; Routledge, M.N.; Akhtar, S.; Riaz, M.; Ramalho, L.N.Z.; de Oliveira, C.A.F.; Ismail, Z. Early life exposure to dietary aflatoxins, health impact and control perspectives: A review. *Trends Food Sci. Technol.* **2021**, *112*, 212–224. [CrossRef]
7. Bonah, E.; Huang, X.; Aheto, J.H.; Osae, R. Application of hyperspectral imaging as a nondestructive technique for foodborne pathogen detection and characterization. *Foodborne Pathog. Dis.* **2019**, *16*, 712–722. [CrossRef] [PubMed]
8. Ngolong Ngea, G.L.; Yang, Q.; Castoria, R.; Zhang, X.; Routledge, M.N.; Zhang, H. Recent trends in detecting, controlling, and detoxifying of patulin mycotoxin using biotechnology methods. *Compr. Rev. Food Sci. Food Saf.* **2020**, *19*, 2447–2472. [CrossRef] [PubMed]
9. Li, H.; Haruna, S.A.; Geng, W.; Wei, W.; Zhang, M.; Ouyang, Q.; Chen, Q. Fabricating a novel colorimetric-bionic sensor coupled multivariate calibration for simultaneous determination of myoglobin proportions in pork. *Sens. Actuators B Chem.* **2021**, *343*, 130181. [CrossRef]
10. Li, Y.; Li, Y.; Zhang, D.; Tan, W.; Shi, J.; Li, Z.; Liu, H.; Yu, Y.; Yang, L.; Wang, X.; et al. A fluorescence resonance energy transfer probe based on functionalized graphene oxide and upconversion nanoparticles for sensitive and rapid detection of zearalenone. *LWT* **2021**, *147*, 111541. [CrossRef]
11. Liu, R.; Ali, S.; Huang, D.; Zhang, Y.; Lü, P.; Chen, Q. A Sensitive Nucleic Acid Detection Platform for Foodborne Pathogens Based on CRISPR-Cas13a System Combined with Polymerase Chain Reaction. *Food Anal. Methods* **2023**, *16*, 356–366. [CrossRef]
12. Zhang, C.; Cui, H.; Han, Y.; Yu, F.; Shi, X. Development of a biomimetic enzyme-linked immunosorbent assay based on molecularly imprinted polymers on paper for the detection of carbaryl. *Food Chem.* **2018**, *240*, 893–897. [CrossRef] [PubMed]
13. Wang, M.; Mohanty, S.K.; Mahendra, S. Nanomaterial-Supported Enzymes for Water Purification and Monitoring in Point-of-Use Water Supply Systems. *Acc. Chem. Res.* **2019**, *52*, 876–885. [CrossRef] [PubMed]
14. Li, Z.; Yang, C.; Lu, W.; Chu, Z.; Zhang, J.; Li, M.; Wang, Q. Ultrasensitive immuno-PCR for detecting aflatoxin B_1 based on magnetic separation and barcode DNA. *Food Control* **2022**, *138*, 109028. [CrossRef]
15. Li, H.; Hassan, M.M.; He, Z.; Haruna, S.A.; Chen, Q.; Ding, Z. A sensitive silver nanoflower-based SERS sensor coupled novel chemometric models for simultaneous detection of chlorpyrifos and carbendazim in food. *LWT* **2022**, *167*, 113804. [CrossRef]
16. Zhu, A.; Ali, S.; Jiao, T.; Wang, Z.; Ouyang, Q.; Chen, Q. Advances in surface-enhanced Raman spectroscopy technology for detection of foodborne pathogens. *Compr. Rev. Food Sci. Food Saf.* **2023**, *22*, 1466–1494. [CrossRef]
17. Abdul Hakeem, D.; Su, S.; Mo, Z.; Wen, H. Upconversion luminescent nanomaterials: A promising new platform for food safety analysis. *Crit. Rev. Food Sci. Nutr.* **2021**, *62*, 8866–8907. [CrossRef]
18. Li, H.; Sheng, W.; Haruna, S.A.; Hassan, M.M.; Chen, Q. Recent advances in rare earth ion-doped upconversion nanomaterials: From design to their applications in food safety analysis. *Compr. Rev. Food Sci. Food Saf.* **2023**, *22*, 3732–3764. [CrossRef]
19. Rong, Y.; Hassan, M.M.; Ouyang, Q.; Chen, Q. Lanthanide ion (Ln^{3+})-based upconversion sensor for quantification of food contaminants: A review. *Compr. Rev. Food Sci. Food Saf.* **2021**, *20*, 3531–3578. [CrossRef] [PubMed]
20. Zhang, L.; Hu, S.; Lu, Y.; Jiang, B.; Liu, X.; Li, X.; Zhao, X.; Yan, X.; Wang, C.; Jia, X.; et al. Photonic Crystal Effects on Upconversion Enhancement of $LiErF_4$:0.5%Tm^{3+}@$LiYF_4$ for Noncontact Cholesterol Detection. *ACS Appl. Mater. Interfaces* **2021**, *14*, 428–438. [CrossRef] [PubMed]
21. Nonat, A.M.; Charbonniere, L.J. Upconversion of light with molecular and supramolecular lanthanide complexes. *Coord. Chem. Rev.* **2020**, *409*, 213192. [CrossRef]
22. Ouyang, Q.; Wang, L.; Ahmad, W.; Rong, Y.; Li, H.; Hu, Y.; Chen, Q. A highly sensitive detection of carbendazim pesticide in food based on the upconversion-MnO_2 luminescent resonance energy transfer biosensor. *Food Chem.* **2021**, *349*, 129157. [CrossRef]
23. Xia, X.; Zhang, B.; Wang, J.; Li, B.; He, K.; Zhang, X. Rapid detection of Escherichia coli O157: H7 by loop-mediated isothermal amplification coupled with a lateral flow assay targeting the z3276 genetic marker. *Food Anal. Method* **2022**, *15*, 908–916. [CrossRef]
24. Farka, Z.; Juřík, T.; Kovář, D.; Trnková, L.; Petr Skládal, P. Nanoparticle-Based Immunochemical Biosensors and Assays: Recent Advances and Challenges. *Chem. Rev.* **2017**, *117*, 9973–10042. [CrossRef] [PubMed]
25. Farka, Z.; Mickert, M.J.; Hlaváček, A.; Skládal, P.; Gorris, H.H. Single Molecule Upconversion-Linked Immunosorbent Assay with Extended Dynamic Range for the Sensitive Detection of Diagnostic Biomarkers. *Anal. Chem.* **2017**, *89*, 11825–11830. [CrossRef] [PubMed]
26. Gorris, H.H.; Soukka, T. What Digital Immunoassays Can Learn from Ambient Analyte Theory: A Perspective. *Anal. Chem.* **2022**, *94*, 6073–6083. [CrossRef]
27. Zhou, Y.; Shao, X.; Han, Y.; Zhang, H. Detection of procalcitonin (PCT) using the double antibody sandwich method based on fluorescence resonance energy transfer between upconversion nanoparticles and quantum dots. *Anal. Methods* **2018**, *10*, 1015–1022. [CrossRef]

28. Chen, C.; Cao, J.; Wang, X.; Chai, Q.; Zhang, Y.; Chen, H.; Zhu, X.; Pan, Y.; Liu, J. A novel dual-flux immunochromatographic test strip based on luminescence resonance energy transfer for simultaneous detection of ochratoxin A and deoxynivalenol. *Microchim. Acta* **2022**, *189*, 466. [CrossRef]
29. Zheng, C.; Yin, M.; Su, B.; Peng, A.; Guo, Z.; Chen, X.; Chen, X. A novel near-infrared light-responsive photoelectrochemical platform for detecting microcystin-LR in fish based on Ag_2S cubes and plasmonic Au nanoparticles. *Talanta* **2021**, *221*, 121447. [CrossRef]
30. Zhang, B.; Sheng, W.; Liu, Y.; Huang, N.; Zhang, W.; Wang, S. Multiplexed fluorescence immunoassay combined with magnetic separation using upconversion nanoparticles as multicolor labels for the simultaneous detection of tyramine and histamine in food samples. *Anal. Chim. Acta* **2020**, *1130*, 117–125. [CrossRef] [PubMed]
31. Chen, Y.; Shen, Y.; Zhao, Y.; Zhu, J.; Wang, H. Rapid detection of zearalenone in cereals using La^{3+}-doped upconversion nanoparticles-based immunochromatographic assay. *Food Control* **2023**, *153*, 109904. [CrossRef]
32. Chen, Y.; Shen, Y.; Wang, H.; Zhang, J.; Zhu, J. A novel dual-channel immunochromatographic strip using up-conversion nanoparticles for simultaneous detection of AFB1 and ZEN in maize. *Anal. Bioanal. Chem.* **2023**, *415*, 4935–4947. [CrossRef]
33. Azam, K.; Akhtar, S.; Gong, Y.Y.; Routledge, M.N.; Ismail, A.; Oliveira, C.A.; Iqbal, S.Z.; Ali, H. Evaluation of the impact of activated carbon-based filtration system on the concentration of aflatoxins and selected heavy metals in roasted coffee. *Food Control* **2021**, *121*, 107583. [CrossRef]
34. Wu, S.; Liu, L.; Duan, N.; Li, Q.; Zhou, Y.; Wang, Z. Aptamer-based lateral flow test strip for rapid detection of zearalenone in corn samples. *J. Agric. Food Chem.* **2018**, *66*, 1949–1954. [CrossRef]
35. Zhang, B.; Li, H.; Pan, W.; Chen, Q.; Ouyang, Q.; Zhao, J. Dual-Color Upconversion Nanoparticles (UCNPs)-Based Fluorescent Immunoassay Probes for Sensitive Sensing Foodborne Pathogens. *Food Anal. Methods* **2016**, *10*, 2036–2045. [CrossRef]
36. Duan, N.; Gong, W.; Wu, S.; Wang, Z. Selection and application of ssDNA aptamers against clenbuterol hydrochloride based on ssDNA library immobilized SELEX. *J. Agric. Food Chem.* **2017**, *65*, 1771–1777. [CrossRef]
37. Yan, C.; Zhang, J.; Yao, L.; Xue, F.; Lu, J.; Li, B.; Chen, W. Aptamer-mediated colorimetric method for rapid and sensitive detection of chloramphenicol in food. *Food Chem.* **2018**, *260*, 208–212. [CrossRef]
38. Ye, F.; Zheng, Y.; Wang, X.; Tan, X.; Zhang, T.; Xin, W.; Wang, J.; Huang, Y.; Fan, Q.; Wang, J. Recognition of Bungarus multicinctus venom by a DNA aptamer against beta-bungarotoxin. *PLoS ONE* **2014**, *9*, e105404. [CrossRef] [PubMed]
39. Li, N.; Zhang, Y.; Wei, T.; Yang, T.; Bao, Q.; Cheng, Q.; Mao, C.; Shuai, Y.; Yang, M. Upconversion nanoparticle-based aptasensor for rapid and ultrasensitive detection of *Staphylococcus aureus* by low-speed centrifugation. *RSC Adv.* **2023**, *13*, 20229–20234. [CrossRef]
40. Cheng, K.; Zhang, J.; Zhang, L.; Wang, L.; Chen, H. Aptamer biosensor for *Salmonella typhimurium* detection based on luminescence energy transfer from Mn^{2+}-doped $NaYF_4$:Yb, Tm upconverting nanoparticles to gold nanorods. *Spectrochim. Acta Part A Mol. Biomol. Spectrosc.* **2017**, *171*, 168–173. [CrossRef] [PubMed]
41. Bonah, E.; Huang, X.; Hongying, Y.; Aheto, J.H.; Yi, R.; Yu, S.; Tu, H. Detection of *Salmonella Typhimurium* contamination levels in fresh pork samples using electronic nose smellprints in tandem with support vector machine regression and metaheuristic optimization algorithms. *J. Food Sci. Technol.* **2021**, *58*, 3861–3870. [CrossRef]
42. Liu, R.; Ali, S.; Haruna, S.A.; Ouyang, Q.; Li, H.; Chen, Q. Development of a fluorescence sensing platform for specific and sensitive detection of pathogenic bacteria in food samples. *Food Control* **2022**, *131*, 108419. [CrossRef]
43. Luo, L.; Liu, X.; Ma, S.; Li, L.; You, T. Quantification of zearalenone in mildewing cereal crops using an innovative photoelectrochemical aptamer sensing strategy based on ZnO-NGQDs composites. *Food Chem.* **2020**, *322*, 126778. [CrossRef]
44. Qiu, H.; Gao, L.; Wang, J.; Pan, J.; Yan, Y.; Zhang, X. A precise and efficient detection of Beta-Cyfluthrin via fluorescent molecularly imprinted polymers with ally fluorescein as functional monomer in agricultural products. *Food Chem.* **2017**, *217*, 620–627. [CrossRef] [PubMed]
45. Mukunzi, D.; Habimana, J.D.D.; Li, Z.; Zou, X. Mycotoxins detection: View in the lens of molecularly imprinted polymer and nanoparticles. *Crit. Rev. Food Sci. Nutr.* **2023**, *63*, 6034–6068. [CrossRef]
46. Lu, Y.; Chen, B.; Yu, M.; Han, J.; Wang, Y.; Tan, Z.; Yan, Y. Simultaneous separation/enrichment and detection of trace ciprofloxacin and lomefloxacin in food samples using thermosensitive smart polymers aqueous two-phase flotation system combined with HPLC. *Food Chem.* **2016**, *210*, 1–8. [CrossRef] [PubMed]
47. Su, X.; Zheng, K.; Tian, X.; Zhou, X.; Zou, X.; Xu, X.; Sun, Z.; Zhang, W. An advanced ratiometric molecularly imprinted sensor based on metal ion reoxidation for indirect and ultrasensitive glyphosate detection in fruit. *Food Chem.* **2023**, *429*, 136927. [CrossRef]
48. Yan, Z.; Fang, G.-Z. Molecularly imprinted polymer based on upconversion nanoparticles for highly selective and sensitive determination of Ochratoxin A. *J. Cent. South Univ.* **2019**, *26*, 515–523. [CrossRef]
49. Yang, W.; Liu, C.; Zhang, B.; Wu, C.; Cao, Y.; Huang, W.; Xu, W. Construction of a Nitrogen-Doped Carbon Quantum Dot Fluorescent Molecularly Imprinted Sensor for Ultra-Sensitive Detection of Sulfadiazine in Pork Samples. *Food Anal. Methods* **2024**, *17*, 1689–1701. [CrossRef]

50. Chen, M.; Pan, L.; Tu, K. A fluorescence biosensor for Salmonella typhimurium detection in food based on the nano-self-assembly of alendronic acid modified upconversion and gold nanoparticles. *Anal. Methods* **2021**, *13*, 2415–2423. [CrossRef]
51. Gao, X.; Yin, Y.; Yan, J.; Zhang, J.; Ma, H.; Zhou, C. Separation, biochemical characterization and salt-tolerant mechanisms of alkaline protease from Aspergillus oryzae. *J. Sci. Food Agric.* **2019**, *99*, 3359–3366. [CrossRef] [PubMed]
52. Yin, M.; Wang, Z.; Xie, P.; Han, L.; Li, L.; Wang, H.; Qiao, X.; Deng, Q. Fluorescence sensing platform for *Cronobacter sakazakii* based on the cationic metal-organic frameworks modified upconversion nanoparticles. *Food Control* **2023**, *145*, 109443. [CrossRef]
53. Li, H.; Bei, Q.; Li, B.; Haruna, S.A.; Marimuthu, M.; Hassan, M.; Ding, Z.; Chen, Q. A novel enzymatic biosensor for CIP in food based on UCNPs and colorimetric strategy of potassium titanium oxalate. *J. Food Compos. Anal.* **2024**, *125*, 105827. [CrossRef]
54. Ouyang, Q.; Wang, L.; Ahmad, W.; Yang, Y.; Chen, Q. Upconversion Nanoprobes Based on a Horseradish Peroxidase-Regulated Dual-Mode Strategy for the Ultrasensitive Detection of *Staphylococcus aureus* in Meat. *J. Agric. Food Chem.* **2021**, *69*, 9947–9956. [CrossRef] [PubMed]
55. Garcia-Vidal, F.J.; Feist, J. Long-distance operator for energy transfer. *Science* **2017**, *357*, 1357–1358. [CrossRef] [PubMed]
56. Jin, B.; Wang, S.; Lin, M.; Jin, Y.; Zhang, S.; Cui, X.; Gong, Y.; Li, A.; Xu, F.; Lu, T.J. Upconversion nanoparticles based FRET aptasensor for rapid and ultrasenstive bacteria detection. *Biosens. Bioelectron.* **2017**, *90*, 525–533. [CrossRef] [PubMed]
57. Wang, F.; Han, Y.; Wang, S.; Ye, Z.; Wei, L.; Xiao, L. Single-Particle LRET Aptasensor for the Sensitive Detection of Aflatoxin B_1 with Upconversion Nanoparticles. *Anal. Chem.* **2019**, *91*, 11856–11863. [CrossRef] [PubMed]
58. Zhang, Z.; Shikha, S.; Liu, J.; Zhang, J.; Mei, Q.; Zhang, Y. Upconversion Nanoprobes: Recent Advances in Sensing Applications. *Anal. Chem.* **2019**, *91*, 548–568. [CrossRef] [PubMed]
59. Li, Y.; Su, R.; Li, H.; Guo, J.; Hildebrandt, N.; Sun, C. Fluorescent Aptasensors: Design Strategies and Applications in Analyzing Chemical Contamination of Food. *Anal. Chem.* **2022**, *94*, 193–224. [CrossRef]
60. Wu, Z.; He, D.; Cui, B. A fluorometric assay for staphylococcal enterotoxin B by making use of platinum coated gold nanorods and of upconversion nanoparticles. *Microchim. Acta* **2018**, *185*, 516. [CrossRef]
61. Li, Y.; Chen, M.; Fan, X.; Peng, J.; Pan, L.; Tu, K.; Chen, Y. Sandwich fluorometric method for dual-role recognition of *Listeria monocytogenes* based on antibiotic-affinity strategy and fluorescence quenching effect. *Anal. Chim. Acta* **2022**, *1221*, 340085. [CrossRef] [PubMed]
62. Han, J.; Wang, L.; Wang, L.; Li, C.; Mao, Y.; Wang, Y. Fabrication of a core-shell-shell magnetic polymeric microsphere with excellent performance for separation and purification of bromelain. *Food Chem.* **2019**, *283*, 1–10. [CrossRef]
63. Kang, Y.; Shi, S.; Sun, H.; Dan, J.; Liang, Y.; Zhang, Q.; Su, Z.; Wang, J.; Zhang, W. Magnetic Nanoseparation Technology for Efficient Control of Microorganisms and Toxins in Foods: A Review. *J. Agric. Food Chem.* **2022**, *70*, 16050–16068. [CrossRef] [PubMed]
64. Hu, Q.; Wu, Q.; Huang, F.; Xu, Z.; Zhou, L.; Zhao, S. Multicolor Coding Up-Conversion Nanoplatform for Rapid Screening of Multiple Foodborne Pathogens. *ACS Appl. Mater. Interfaces* **2021**, *13*, 26782–26789. [CrossRef] [PubMed]
65. Shi, C.; Chen, Y.; Li, C.; Al-Asmari, F.; Cui, H.; Lin, L. Potential Application of *Lactiplantibacillus plantarum* in Food Bio-preservation–A Comprehensive Review with a Focus on the Antibacterial and Anti-Virulence Effects on Foodborne Pathogens. *Food Rev. Int.* **2024**, *40*, 2993–3019. [CrossRef]
66. Chen, M.; Song, Y.; Han, L.; Zhou, D.; Wang, Y.; Pan, L.; Tu, K. An Ultrasensitive Upconversion Fluorescence Aptasensor Based on Graphene Oxide Release and Magnetic Separation for *Staphylococcus aureus* Detection. *Food Anal. Methods* **2022**, *15*, 2791–2800. [CrossRef]
67. Zhang, P.; Zhang, Y.; Lin, Q.; Yao, H.; Wei, T. Principle and the Research Progress of Fluorescent Chemosensors for Cations Recognition. *Chin. J. Org. Chem.* **2014**, *34*, 1300. [CrossRef]
68. Gao, Y.; Yu, Z.; Huang, L.; Zeng, Y.; Liu, X.; Tang, D. Photoinduced Electron Transfer Modulated Photoelectric Signal: Toward an Organic Small Molecule-Based Photoelectrochemical Platform for Formaldehyde Detection. *Anal. Chem.* **2023**, *95*, 9130–9137. [CrossRef] [PubMed]
69. Ouyang, Q.; Zhang, M.; Yang, Y.; Din, Z.-U.; Chen, Q. Mesoporous silica-modified upconversion biosensor coupled with real-time ion release properties for ultrasensitive detection of *Staphylococcus aureus* in meat. *Food Control* **2023**, *145*, 109444. [CrossRef]
70. Pan, W.; Zhao, J.; Chen, Q. Fabricating Upconversion Fluorescent Probes for Rapidly Sensing Foodborne Pathogens. *J. Agric. Food Chem.* **2015**, *63*, 8068–8074. [CrossRef] [PubMed]
71. Yang, N.; Wang, P.; Xue, C.Y.; Sun, J.; Mao, H.P.; Oppong, P.K. A portable detection method for organophosphorus and carbamates pesticide residues based on multilayer paper chip. *J. Food Process Eng.* **2018**, *41*, e12867. [CrossRef]
72. Huang, X.; Lv, R.; Wang, S.; Aheto, J.H.; Dai, C. Integration of computer vision and colorimetric sensor array for nondestructive detection of mango quality. *J. Food Process Eng.* **2018**, *41*, e12873. [CrossRef]
73. Wu, J.; Wu, J.; Wei, W.; Zhang, Y.; Chen, Q. Upconversion Nanoparticles Based Sensing: From Design to Point-of-Care Testing. *Small* **2024**, *20*, 2311729. [CrossRef] [PubMed]
74. Wu, S.; Liu, L.; Duan, N.; Wang, W.; Yu, Q.; Wang, Z. A test strip for ochratoxin A based on the use of aptamer-modified fluorescence upconversion nanoparticles. *Microchim. Acta* **2018**, *185*, 497. [CrossRef] [PubMed]

75. Li, H.; Ahmad, W.; Rong, Y.; Chen, Q.; Zuo, M.; Ouyang, Q.; Guo, Z. Designing an aptamer based magnetic and upconversion nanoparticles conjugated fluorescence sensor for screening *Escherichia coli* in food. *Food Control* **2020**, *107*, 106761. [CrossRef]
76. Zhang, Y.; Zhao, C.; Guo, Z.; Yang, T.; Zhang, X.; Huang, X.; Shi, J.; Gao, S.; Zou, X. Ultrasensitive analysis of *Escherichia coli* O157: H7 based on immunomagnetic separation and labeled surface-enhanced Raman scattering with minimized false positive identifications. *J. Agric. Food Chem.* **2024**, *72*, 22349–22359. [CrossRef]
77. Guo, L.; Azam, S.R.; Guo, Y.; Liu, D.; Ma, H. Germicidal efficacy of the pulsed magnetic field against pathogens and spoilage microorganisms in food processing: An overview. *Food Control* **2022**, *136*, 108496. [CrossRef]
78. Duan, N.; Chang, B.; Zhang, H.; Wang, Z.; Wu, S. *Salmonella typhimurium* detection using a surface-enhanced Raman scattering-based aptasensor. *Int. J. Food Microbiol.* **2016**, *218*, 38–43. [CrossRef]
79. Wu, S.; Duan, N.; Qiu, Y.; Li, J.; Wang, Z. Colorimetric aptasensor for the detection of *Salmonella enterica serovar typhimurium* using $ZnFe_2O_4$-reduced graphene oxide nanostructures as an effective peroxidase mimetic. *Int. J. Food Microbiol.* **2017**, *261*, 42–48. [CrossRef]
80. Song, Y.; Chen, M.; Han, L.; Yan, Z.; Pan, L.; Tu, K. A novel ADA-coated UCNPs@NB sensing platform combined with nucleic acid amplification for rapid detection of *Escherichia coli*. *Anal. Chim. Acta* **2023**, *1239*, 340751. [CrossRef]
81. Yin, M.; Jing, C.; Li, H.; Deng, Q.; Wang, S. Surface chemistry modified upconversion nanoparticles as fluorescent sensor array for discrimination of foodborne pathogenic bacteria. *J. Nanobiotechnol.* **2020**, *18*, 41. [CrossRef]
82. Liu, R.; Zhang, Y.; Ali, S.; Haruna, S.A.; He, P.; Li, H.; Ouyang, Q.; Chen, Q. Development of a fluorescence aptasensor for rapid and sensitive detection of *Listeria monocytogenes* in food. *Food Control* **2021**, *122*, 107808. [CrossRef]
83. Cui, H.; Zhang, C.; Li, C.; Lin, L. Inhibition mechanism of cardamom essential oil on methicillin-resistant *Staphylococcus aureus* biofilm. *LWT* **2020**, *122*, 109057. [CrossRef]
84. Li, H.; Li, C.; Shi, C.; Alharbi, M.; Cui, H.; Lin, L. Phosphoproteomics analysis reveals the anti-bacterial and anti-virulence mechanism of eugenol against *Staphylococcus aureus* and its application in meat products. *Int. J. Food Microbiol.* **2024**, *414*, 110621. [CrossRef]
85. Zdeněk Farka, Z.; Juřík, T.; Pastucha, M.; Skládal, P. Enzymatic Precipitation Enhanced Surface Plasmon Resonance Immunosensor for the Detection of Salmonella in Powdered Milk. *Anal. Chem.* **2016**, *88*, 24.
86. Chen, M.; Han, L.; Zhou, D.; Kong, L.; Pan, L.; Tu, K. Amplified UCNPs-Mitoxantrone dihydrochloride fluorescence PCR sensor based on inner filter for ultrasensitive and rapid determination of *Salmonella typhimurium*. *Sens. Actuators B Chem.* **2022**, *355*, 131287. [CrossRef]
87. Ren, X.; Zhang, Q.; Wu, W.; Yan, T.; Tang, X.; Zhang, W.; Yu, L.; Li, P. Anti-idiotypic nanobody-phage display-mediated real-time immuno-PCR for sensitive, simultaneous and quantitative detection of total aflatoxins and zearalenone in grains. *Food Chem.* **2019**, *297*, 124912. [CrossRef]
88. Wang, C.; Zhao, X.; Gu, C.; Xu, F.; Zhang, W.; Huang, X.; Qian, J. Fabrication of a versatile aptasensing chip for aflatoxin B1 in photothermal and electrochemical dual modes. *Food Anal. Methods* **2022**, *15*, 3390–3399. [CrossRef]
89. Shen, L.; Wang, Y.; Li, X.; Hou, Z.; Mao, J.; Shi, J.; Battino, M.; Routledge, M.N.; Gong, Y.; Zou, X.; et al. Spatial-temporal distribution of deoxynivalenol, aflatoxin B_1, and zearalenone in the solid-state fermentation basin of traditional vinegar and their potential correlation with microorganisms. *Food Chem.* **2024**, *433*, 137317. [CrossRef] [PubMed]
90. Li, Y.; Kong, W.; Li, M.; Liu, H.; Zhao, X.; Yang, S.; Yang, M. Litsea cubeba essential oil as the potential natural fumigant: Inhibition of *Aspergillus flavus* and AFB_1 production in licorice. *Ind. Crops Prod.* **2016**, *80*, 186–193. [CrossRef]
91. Chen, Z.; Lin, H.; Wang, F.; Adade, S.Y.S.S.; Peng, T.; Chen, Q. Discrimination of toxigenic and non-toxigenic *Aspergillus flavus* in wheat based on nanocomposite colorimetric sensor array. *Food Chem.* **2024**, *430*, 137048. [CrossRef] [PubMed]
92. Xie, G.; Zhu, M.; Liu, Z.; Zhang, B.; Shi, M.; Wang, S. Development and evaluation of the magnetic particle-based chemiluminescence immunoassay for rapid and quantitative detection of Aflatoxin B_1 in foodstuff. *Food Agric. Immunol.* **2018**, *29*, 564–576. [CrossRef]
93. Sun, C.; Li, H.; Koidis, A.; Chen, Q. Quantifying Aflatoxin B_1 in peanut oil using fabricating fluorescence probes based on upconversion nanoparticles. *Spectrochim. Acta Part A Mol. Biomol. Spectrosc.* **2016**, *165*, 120–126. [CrossRef] [PubMed]
94. Xu, Z.; Li, Q.X.; Zhang, L.W.; Chen, M.L.; Tu, J.; Chen, W.; Zhu, Y.Y.; Cheng, Y.H. Target-modulated UCNPs-AChE assembly equipped with microenvironment-responsive immunosensor. *Sens. Actuators B Chem.* **2022**, *352*, 131050. [CrossRef]
95. Godana, E.A.; Yang, Q.; Wang, K.; Zhang, H.; Zhang, X.; Zhao, L.; Abdelhai, M.H.; Legrand, N.N.G. Bio-control activity of Pichia anomala supplemented with chitosan against *Penicillium expansum* in postharvest grapes and its possible inhibition mechanism. *LWT* **2020**, *124*, 109188. [CrossRef]
96. Wang, Y.; Yang, Q.; Godana, E.A.; Zhang, Y.; Zhang, H. Ultrastructural observation and transcriptome analysis provide insights into mechanisms of *Penicillium expansum* invading apple wounds. *Food Chem.* **2023**, *414*, 135633. [CrossRef]
97. Apaliya, M.T.; Zhang, H.; Zheng, X.; Yang, Q.; Mahunu, G.K.; Kwaw, E. Exogenous trehalose enhanced the biocontrol efficacy of Hanseniaspora uvarum against grape berry rots caused by *Aspergillus tubingensis* and *Penicillium commune*. *J. Sci. Food Agric.* **2018**, *98*, 4665–4672. [CrossRef] [PubMed]

98. Wang, K.; Ngea, G.L.N.; Godana, E.A.; Shi, Y.; Lanhuang, B.; Zhang, X.; Zhao, L.; Yang, Q.; Wang, S.; Zhang, H. Recent advances in *Penicillium expansum* infection mechanisms and current methods in controlling *P. expansum* in postharvest apples. *Crit. Rev. Food Sci. Nutr.* **2023**, *63*, 2598–2611. [CrossRef]
99. Lin, H.; Wang, F.; Lin, J.; Yang, W.; Kang, W.; Jiang, H.; Adade, S.Y.S.S.; Cai, J.; Xue, Z.; Chen, Q. Detection of wheat toxigenic *aspergillus flavus* based on nano-composite colorimetric sensing technology. *Food Chem.* **2023**, *405*, 134803. [CrossRef] [PubMed]
100. Wei, M.; Dhanasekaran, S.; Yang, Q.; Ngea, G.L.N.; Godana, E.A.; Zhang, H. Degradation and stress response mechanism of *Cryptococcus podzolicus* Y3 on ochratoxin A at the transcriptional level. *LWT* **2022**, *157*, 113061. [CrossRef]
101. Wang, Y.; Liu, F.; Wang, L.; Wang, Q.; Selvaraj, J.N.; Zhao, Y.; Wang, Y.; Xing, F.; Liu, Y. pH-signaling transcription factor AopacC regulates ochratoxin A biosynthesis in Aspergillus ochraceus. *J. Agric. Food Chem.* **2018**, *66*, 4394–4401. [CrossRef] [PubMed]
102. Wei, M.; Dhanasekaran, S.; Godana, E.A.; Yang, Q.; Sui, Y.; Zhang, X.; Ngea, G.L.N.; Zhang, H. Whole-genome sequencing of *Cryptococcus podzolicus* Y3 and data-independent acquisition-based proteomic analysis during OTA degradation. *Food Control* **2022**, *136*, 108862. [CrossRef]
103. Zhang, H.; Apaliya, M.T.; Mahunu, G.K.; Chen, L.; Li, W. Control of ochratoxin A-producing fungi in grape berry by microbial antagonists: A review. *Trends Food Sci. Technol.* **2016**, *51*, 88–97. [CrossRef]
104. Shang, L.; Bai, X.; Chen, C.; Liu, L.; Li, M.; Xia, X.; Wang, Y. Isolation and identification of a *Bacillus megaterium* strain with ochratoxin A removal ability and antifungal activity. *Food Control* **2019**, *106*, 106743. [CrossRef]
105. Dai, S.; Wu, S.; Duan, N.; Chen, J.; Zheng, Z.; Wang, Z. An ultrasensitive aptasensor for Ochratoxin A using hexagonal core/shell upconversion nanoparticles as luminophores. *Biosens. Bioelectron.* **2017**, *91*, 538–544. [CrossRef]
106. Jin, Z.; Sheng, W.; Huang, N.; Ren, L.; Sun, M.; Bai, D.; Wang, S.; Wang, Z.; Tang, X.; Ya, T. Blue-green-red multicolor upconversion nanoparticles based fluorescence immunoassay for simultaneous detection of three mycotoxins in cereals. *Microchem. J.* **2023**, *193*, 109181. [CrossRef]
107. Wu, S.; Duan, N.; Li, X.; Tan, G.; Ma, X.; Xia, Y.; Wang, Z.; Wang, H. Homogenous detection of fumonisin B_1 with a molecular beacon based on fluorescence resonance energy transfer between $NaYF_4$: Yb, Ho upconversion nanoparticles and gold nanoparticles. *Talanta* **2013**, *116*, 611–618. [CrossRef] [PubMed]
108. Xu, S.; Wang, Y.; Hu, J.; Chen, X.; Qiu, Y.; Shi, J.; Wang, G.; Xu, J. Isolation and characterization of *Bacillus amyloliquefaciens* MQ01, a bifunctional biocontrol bacterium with antagonistic activity against *Fusarium graminearum* and biodegradation capacity of zearalenone. *Food Control* **2021**, *130*, 108259. [CrossRef]
109. Godana, E.A.; Yang, Q.; Zhang, X.; Zhao, L.; Wang, K.; Dhanasekaran, S.; Mehari, T.G.; Zhang, H. Biotechnological and biocontrol approaches for mitigating postharvest diseases caused by fungal pathogens and their mycotoxins in fruits: A review. *J. Agric. Food Chem.* **2023**, *71*, 17584–17596. [CrossRef]
110. He, D.; Wu, Z.; Cui, B.; Jin, Z.; Xu, E. A fluorometric method for aptamer-based simultaneous determination of two kinds of the fusarium mycotoxins zearalenone and fumonisin B_1 making use of gold nanorods and upconversion nanoparticles. *Microchim. Acta* **2020**, *187*, 254. [CrossRef]
111. Douglass, M. Lateral Flow Assay for Deoxynivalenol in Barley: An ASBC Collaborative Subcommittee Report. *J. Am. Soc. Brew. Chem.* **2019**, *77*, 69–70. [CrossRef]
112. Li, Y.; Liu, G.; Fu, X.; He, J.; Wang, Z.; Hou, J.; Cao, X.; Shi, W.; Zhang, S. High-Sensitive Chemiluminescent ELISA Method Investigation for the Determination of Deoxynivalenol in Rice. *Food Anal. Methods* **2014**, *8*, 656–660. [CrossRef]
113. Zhang, X.; Yu, X.; Wang, J.; Wang, Q.; Meng, H.; Wang, Z. One-step core/multishell quantum dots-based fluoroimmunoassay for screening of deoxynivalenol in maize. *Food Anal. Methods* **2018**, *11*, 2569–2578. [CrossRef]
114. You, F.; Wen, Z.; Yuan, R.; Qian, J.; Long, L.; Wang, K. Sensitive and stable detection of deoxynivalenol based on electrochemiluminescence aptasensor enhanced by 0D/2D homojunction effect in food analysis. *Food Chem.* **2023**, *403*, 134397. [CrossRef]
115. Lin, X.; Li, C.; Meng, X.; Yu, W.; Duan, N.; Wang, Z.; Wu, S. CRISPR-Cas12a-mediated luminescence resonance energy transfer aptasensing platform for deoxynivalenol using gold nanoparticle-decorated $Ti_3C_2T_x$ MXene as the enhanced quencher. *J. Hazard. Mater.* **2022**, *433*, 128750. [CrossRef]
116. Chen, Q.; Hu, W.; Sun, C.; Li, H.; Ouyang, Q. Synthesis of improved upconversion nanoparticles as ultrasensitive fluorescence probe for mycotoxins. *Anal. Chim. Acta* **2016**, *938*, 137–145. [CrossRef]
117. Fang, X.; Liu, T.; Xue, C.; Xue, G.; Wu, M.; Liu, P.; Hammock, B.D.; Lai, W.; Peng, J.; Zhang, C. Competitive ratiometric fluorescent lateral flow immunoassay based on dual emission signal for sensitive detection of chlorothalonil. *Food Chem.* **2024**, *433*, 137200. [CrossRef] [PubMed]
118. Ju, Q.; Noor, M.O.; Krull, U.J. Paper-based biodetection using luminescent nanoparticles. *Analyst* **2016**, *141*, 2838–2860. [CrossRef] [PubMed]
119. Teepoo, S.; Wongtongdee, U.; Phapugrangkul, P. Development of qualitative and quantitative immunochromatographic strip test assay for rapid and simple detection of leucomalachite green residual in aquatic animals. *Food Chem.* **2020**, *320*, 126613. [CrossRef] [PubMed]

120. Liu, Y.; Liu, D.; Cui, S.; Li, C.; Yun, Z.; Zhang, J.; Sun, F. Design of a Signal-Amplified Aptamer-Based Lateral Flow Test Strip for the Rapid Detection of Ochratoxin A in Red Wine. *Foods* **2022**, *11*, 1598. [CrossRef]
121. Mi, F.; Hu, C.; Wang, Y.; Wang, L.; Peng, F.; Geng, P.; Guan, M. Recent advancements in microfluidic chip biosensor detection of foodborne pathogenic bacteria: A review. *Anal. Bioanal. Chem.* **2022**, *414*, 2883–2902. [CrossRef]
122. Shang, Y.; Xiang, X.; Ye, Q.; Wu, Q.; Zhang, J.; Lin, J.M. Advances in nanomaterial-based microfluidic platforms for on-site detection of foodborne bacteria. *TrAC Trends Anal. Chem.* **2022**, *147*, 116509. [CrossRef]
123. Wang, Y.; Mao, H.; Zhang, X.; Liu, Y.; Du, X. A rapid detection method for tomato Gray mold spores in greenhouse based on microfluidic chip enrichment and lens-less diffraction image processing. *Foods* **2021**, *10*, 3011. [CrossRef] [PubMed]
124. Chen, Y.; Meng, X.; Zhu, Y.; Shen, M.; Lu, Y.; Cheng, J.; Xu, Y. Rapid detection of four mycotoxins in corn using a microfluidics and microarray-based immunoassay system. *Talanta* **2018**, *186*, 299–305. [CrossRef] [PubMed]
125. Zhang, M.; Wang, X.; Liu, S.; Riaz, T.; Chen, Q.; Ouyang, Q. Integrating target-responsive microfluidic-based biosensing chip with smartphone for simultaneous quantification of multiple fluoroquinolones. *Biosens. Bioelectron.* **2024**, *254*, 116192. [CrossRef]
126. Yin, L.; Cai, J.; Ma, L.; You, T.; Arslan, M.; Jayan, H.; Zou, X.; Gong, Y. Dual function of magnetic nanocomposites-based SERS lateral flow strip for simultaneous detection of aflatoxin B_1 and zearalenone. *Food Chem.* **2024**, *446*, 138817. [CrossRef] [PubMed]
127. Wang, J.; Gao, Z.; Zhang, Y.; Zhou, J.; Wu, J.; Li, P. Real-time detection and location of potted flowers based on a ZED camera and a YOLO V4-tiny deep learning algorithm. *Horticulturae* **2021**, *8*, 21. [CrossRef]
128. Yin, L.; You, T.; El-Seedi, H.R.; El-Garawani, I.M.; Guo, Z.; Zou, X.; Cai, J. Rapid and sensitive detection of zearalenone in corn using SERS-based lateral flow immunosensor. *Food Chem.* **2022**, *396*, 133707. [CrossRef]
129. Lin, X.; Li, C.; Tong, X.; Duan, N.; Wang, Z.; Wu, S. A portable paper-based aptasensor for simultaneous visual detection of two mycotoxins in corn flour using dual-color upconversion nanoparticles and Cu-TCPP nanosheets. *Food Chem.* **2023**, *404*, 134750. [CrossRef] [PubMed]
130. Zheng, C.; Yin, M.; Ge, R.; Wei, J.; Su, B.; Chen, X.; Chen, X. Competitive near-infrared PEC immunosorbent assay for monitoring okadaic acid based on a disposable flower-like WO_3-Modified screen-printed electrode. *Biosens. Bioelectron.* **2021**, *185*, 113278. [CrossRef]
131. Dong, X.; Huang, A.; He, L.; Cai, C.; You, T. Recent advances in foodborne pathogen detection using photoelectrochemical biosensors: From photoactive material to sensing strategy. *Front. Sustain. Food Syst.* **2024**, *8*, 1432555. [CrossRef]
132. Wu, B.; Tang, W.; Zhou, J.; Jia, H.; Shen, H.; Qi, Z. Near-infrared spectroscopy combined with fuzzy fast pseudoinverse linear discriminant analysis to discriminate mee tea grades. *Heliyon* **2024**, *10*, e27732. [CrossRef]
133. Yin, M.; Liu, C.; Ge, R.; Fang, Y.; Wei, J.; Chen, X.; Chen, Q.; Chen, X. Paper-supported near-infrared-light-triggered photoelectrochemical platform for monitoring *Escherichia coli* O157:H7 based on silver nanoparticles-sensitized-upconversion nanophosphors. *Biosens. Bioelectron.* **2022**, *203*, 114022. [CrossRef]
134. Bonah, E.; Huang, X.; Aheto, J.H.; Osae, R. Application of electronic nose as a non-invasive technique for odor fingerprinting and detection of bacterial foodborne pathogens: A review. *J. Food Sci. Technol.* **2020**, *57*, 1977–1990. [CrossRef]
135. Gong, Y.; Zheng, Y.; Jin, B.; You, M.; Wang, J.; Li, X.; Lin, M.; Xu, F.; Li, F. A portable and universal upconversion nanoparticle-based lateral flow assay platform for point-of-care testing. *Talanta* **2019**, *201*, 126–133. [CrossRef] [PubMed]
136. Farka, Z.; Vytiskova, K.; Makhneva, E.; Zikmundova, E.; Holub, D.; Buday, J.; Prochazka, D.; Novotny, K.; Skladal, P.; Porizka, P.; et al. Comparison of single and double pulse laser-induced breakdown spectroscopy for the detection of biomolecules tagged with photon-upconversion nanoparticles. *Anal. Chim. Acta* **2024**, *1299*, 342418. [CrossRef] [PubMed]
137. Lunkenheimer, P.; Emmert, S.; Gulich, R.; Köhler, M.; Wolf, M.; Schwab, M.; Loidl, A. Electromagnetic-radiation absorption by water. *Phys. Rev. E* **2017**, *96*, 062607. [CrossRef]
138. Hlaváček, A.; Farka, Z.; Mickert, M.J.; Kostiv, U.; Brandmeier, J.C.; Horák, D.; Skládal, P.; Foret, F.; Gorris, H.H. Bioconjugates of photon-upconversion nanoparticles for cancer biomarker detection and imaging. *Nat. Protocols. Nat.* **2022**, *17*, 1028–1072. [CrossRef]

Disclaimer/Publisher's Note: The statements, opinions and data contained in all publications are solely those of the individual author(s) and contributor(s) and not of MDPI and/or the editor(s). MDPI and/or the editor(s) disclaim responsibility for any injury to people or property resulting from any ideas, methods, instructions or products referred to in the content.